Title: Sedimentary ancient DNA shows terrestrial plant richness continuously increased over the Holocene in northern Fennoscandia

Short title: Holocene plant diversity in Fennoscandia

Authors: Dilli P. Rijal,[1,2*†] Peter D. Heintzman,[1*†] Youri Lammers,[1] Nigel G. Yoccoz,[2] Kelsey E. Lorberau,[2] Iva Pitelkova,[1] Tomasz Goslar,[3] Francisco J.A. Murguzur,[2], J. Sakari Salonen,[4] Karin F. Helmens,[5,6] Jostein Bakke,[7] Mary E. Edwards,[1,8] Torbjørn Alm,[1] Kari A. Bråthen,[2] Antony G. Brown,[1,8] Inger G. Alsos[1*†]

[1] The Arctic University Museum of Norway, UiT - The Arctic University of Norway, Tromsø, Norway.

[2] Department of Arctic and Marine Biology, UiT - The Arctic University of Norway, Tromsø, Norway.

[3] Faculty of Physics, Adam Mickiewicz University, Poznań, Poland.

[4]Department of Geosciences and Geography, University of Helsinki, Finland.

[5]Swedish Museum of Natural History, P.O. Box 50007, 10405 Stockholm, Sweden.

[6] Värriö Research Station, Institute for Atmospheric and Earth System Research INAR/Physics, P.O. Box 64, 00014 University of Helsinki, Finland.

[7] Department of Earth Science, University of Bergen, Norway.

[8] School of Geography and Environmental Science, University of Southampton, UK Southampton.

[*]Dilli P. Rijal (dilliprijal@gmail.com), Peter D. Heintzman (peter.d.heintzman@uit.no), Inger G. Alsos (inger.g.alsos@uit.no).

[†]These authors contributed equally to this work.

Abstract

The effects of climate change on species richness is debated but can be informed by the past. Here, we assess the impact of Holocene climate changes and nutrients on terrestrial plant richness across multiple sites from northern Fennoscandia using new sedimentary ancient DNA (*sed*aDNA) data quality control methods. We find that richness increased steeply during the rapidly warming Early Holocene. In contrast to findings from most pollen studies, we show that richness continued to increase through the Middle to Late Holocene even though temperature decreased, with the regional species pool only stabilizing during the last two millennia. Furthermore, overall increase in richness was greater in catchments with higher soil nutrient availability. We suggest that richness will rapidly increase with ongoing warming, especially at localities with high nutrient availability and even in the absence of increased human activity in the region, although delays of millennia may be expected.

Introduction

Our ability to counter the current loss of biodiversity is dependent on how well we understand the causes of its change through time. However, the trajectory of biodiversity, especially in response to ongoing climate change, is vigorously debated (*1*, *2*), with discrepancy among short-term biodiversity patterns at global, regional, and local scales, whereby local processes may compensate or even counteract global trends (*3*). Our understanding of how species pools - the accumulated species richness at a given spatiotemporal scale (sensu *4*) - affect biodiversity patterns through time is limited, in part because constructing past species pools from present-day data is a non-trivial task (*5*).

The largest impact of ongoing climate change is expected to be at high latitudes (*6*). Field and modelling analyses suggest plant species richness will increase at high latitudes in Europe as summer temperature increases (*7*). Short-term observational studies, however, suggest that colonization by terrestrial species is lagging behind shifts in temperature isotherms (*8*), which can be compensated in the short term by local extinction lags (*1*). Therefore, studies addressing species pools and local richness at high latitudes and at different spatiotemporal scales are warranted to increase our understanding of biodiversity responses to ongoing climate change.

Changes in species richness by other drivers, such as nutrient levels, species introductions, and dispersal lags, are often context-dependent and hence difficult to predict. For example, edaphic variation, including variation in nutrient content, is hypothesized to strongly influence establishment, ecological drift, and niche selection, which all affect the local species pool, and this in turn affects richness (*9*). Experimental approaches have shown a non-linear impact of fertilization on Arctic plant richness and their ecosystem functions (*10*). An overall greater species richness has been reported from calcareous as compared with siliceous bedrock areas in the European Alps and northern Fennoscandia, whereby leaching of the former produces neutral to acidic microenvironments, providing a mosaic of habitats that may promote species establishment and an increase local richness (*11*, *12*). Human land

use may also increase soil fertility and thereby richness (*13*), but the overall human impact at high latitudes in Europe is low (*14*). There is also evidence that the trajectory of succession, particularly soil formation, after glacier retreat varies due to abiotic rather than biotic factors (*15*). Furthermore, it has been found that regional plant species richness in previously glaciated regions may still be responding to past deglaciation, whereas local richness may be determined by local habitat factors (*16*).

There is a clear need for long-term data at the regional and local scales to better understand biodiversity trends (*17*). Paleoecological studies, especially those based on pollen (palynological) analyses, provide direct long-term evidence of plant biodiversity change and have been widely used to estimate effects of climate changes on richness (*18–20*). Contrasting richness patterns have been observed in different regions over the Holocene (11.7 thousand calibrated years before present (ka) to recent). In the European northern boreal region (Scotland, Fennoscandia, Iceland, Baltic States, NW Russia) pollen richness shows an overall decrease from 11.7-7.0 ka, followed by an increase to nearly peak levels by recent times (*19*). In the far north of Fennoscandia, however, a study spanning a forest to shrub-tundra gradient shows an inconsistent richness pattern through the Holocene (*21*). If plant dispersal had been slow, due to not being able to track a changing climate as it changes (dispersal lag) for example, then diversity in previously glaciated areas would be expected to increase over time. Such a scenario was not observed in central Sweden (*22*) but was inferred in Norway (*20*). These studies highlight the challenges of comparing pollen richness across different vegetation zones, which is confounded by inferences based on pollen being impacted by over-abundance of a few taxa (swamping), under-representation of other taxa, or low abundance of all taxa, the latter of which is a particular problem above the treeline (*23*).

An alternative, emerging proxy for examining long term, regional scale richness and species pool trends is sedimentary ancient DNA (*sed*aDNA). Compared to pollen, *sed*aDNA provides higher taxonomic resolution, has fewer problems with swamping, and is considered to only represent the local

plant community (*24–26*). In a small catchment, *sed*aDNA may, therefore, also register the effect of drivers on a local rather than regional scale (*27*). Ground truthing studies show a strong correlation between modern sedimentary DNA-inferred richness and richness of modern vegetation around lake catchments (*28*). However, in contrast to pollen, *sed*aDNA studies have focused almost exclusively on single sites (but see *27*, *29*, *30*), thereby limiting our spatial understanding of richness and species pool patterns. A key challenge to combining multi-site *sed*aDNA data from lake cores is that data need to be directly comparable, both within (temporal) and between (spatial) sites, otherwise biased richness estimates resulting from data quality problems could potentially lead to erroneous local- and regional-scale inferences.

Here, we generate the largest *sed*aDNA data set to date, consisting of 387 dated samples from 10 sites in northern Fennoscandia using vascular plant metabarcoding, and harmonize the entire data set using standardized taxonomy and novel data quality control measures that will be highly applicable to the wider environmental DNA community. Capitalizing on this harmonized high resolution taxonomic data set, we estimate richness, local species pools (accumulated richness per catchment), and the regional species pool (accumulated richness for all 10 sites) throughout the Holocene which we compare to two potential drivers, climate and local edaphic conditions. We find that temperature and soil nutrients are important drivers, but suggest that dispersal lags and habitat diversification also provide an important mechanism for plant richness changes through time. By providing refined paleoecological insights, sedaDNA data are well positioned to increase the precision of integrative ecological models for predicting the consequences of ongoing climate change.

Results

Age-depth models

We constructed Bayesian age-depth models for 10 lake sites (Figs. 1, 2, S1) to estimate the age of each individual *sed*aDNA sample. Since the cores were all central or near-central lake locations and the

lakes were medium to small with in most cases only one depositional basin, the age-depth curves were approximately linear or curvilinear with three exceptions (Figs. 2, S1). Kuutsjärvi had a distinct reduction in sedimentation rate from around 4.0 ka. Sandfjorddalen had stepped changes in the sedimentation rate with possible hiatuses in the Early Holocene (11.0-8.0 ka) and Late Holocene between 6.0 and 2.0 ka. This probably reflects its position in the valley floor as a flow-through lake. Lastly, Sierravannet had a distinct upturn in the accumulation rate around 0.6 ka to present, which occurs after a putative flood event at ca. 48-40 cm composite depth (equivalent to ca. 0.6 ka). This 8 - cm layer is characterised by a dark band in the visible stratigraphy, a rapid decrease and then increase in organic carbon (loss-on-ignition, LOI), and two older-than-expected dates, which were consequently not included in the age-depth model. Given that this lake has the largest catchment area and there is a change in lithology, this is probably the result of flooding from the upstream lakes and fluvial network. The terrestrial plant taxonomic richness trends are unaffected by the removal of the four *sed*aDNA samples that fall within this flood event window (Fig. S2). For the interpretation of the *sed*aDNA records, the age-depth models provided similar temporal resolution of 158-616 years per sample for all lakes except Sierravannet, which had 63 years per sample. Six of the sedimentary records covered the entire Holocene (Figs. 2, S1) and all except one (Sierravannet) covered the three periods of the Holocene (Early, 11.7-8.3 ka; Middle, 8.3-4.25 ka; Late Holocene, 4.25-0.0 ka), although the usable Nesservatnet record was reduced to the Late Holocene after removal of low quality *sed*aDNA samples (see below). For two records that extend into the lateglacial (late Pleistocene; Langfjordvannet, Nordvivatnet), the age-depth models are not well constrained in the lateglacial period. For Langfjordvannet, three hiatuses were inferred by Otterå (*31*). We tentatively infer a single hiatus for Nordvivatnet (Fig. 2), which could have been caused by a rock slide, and is based on the recovery of glacially-scarred stones (impressions shown in visible stratigraphy in Fig. S1H), low organic carbon (LOI), and comparable radiocarbon dates.

130

131 Sedimentary ancient DNA data quality assessment

132 Across our 10 lake sediment records, we generated 91.6 million raw sequence reads from 387 sediment
133 samples and 90 control samples. We observed notable differences in data quality between samples both
134 within and between lake records during preliminary data exploration. We therefore sought to develop
135 criteria to scrutinize the quality of samples and provide a cut-off for removing those considered
136 problematic and which may have been impacted by poor DNA quality or methodological issues, such
137 as extract inhibition. We developed two statistics based on the most read-abundant sequences, with the
138 rationale that if these sequences were not replicable, then we cannot exclude methodological problems.
139 We first developed a *metabarcoding technical quality (MTQ)* score to assess metabarcoding success on
140 a per-sample basis. This score is the proportion of positive PCR detections across the 10 most read-
141 abundant sequences within a sample prior to any taxonomic identification. We next developed a
142 *metabarcoding analytical quality (MAQ)* score to assess the success of recovering sequences of
143 interest. This score is the same as the *MTQ* score, except that the 10 most read-abundant and
144 taxonomically-identified sequences, after removing those that matched the *blacklists*, were used.
145 Sources of *MTQ* and *MAQ* score divergence include the co-amplification of unidentified and/or
146 contaminant sequences. For all samples across the data set, we examined the distribution of *MTQ* and
147 *MAQ* scores and used these to infer that samples should require an *MTQ* score of ≥0.75 and *MAQ* score
148 of ≥0.2 to pass quality control (QC) and be included in downstream analyses (Figs. 3, S3, S4). This
149 cutoff excluded all negative controls, which had an *MTQ* score of <0.75 and *MAQ* score of <0.1.
150 After applying our QC thresholds and removing duplicates, we retained 316 samples (Fig. 3).
151 This resulted in 12-55 samples retained per record (Data sets S4, S8; Fig. S3). We retained 402
152 barcodes, which were collapsed to 346 taxa with between 89-200 taxa recorded from each lake record
153 (Table S1). Of these, 50% could be assigned to the species level (Data sets S6, S7). As our focus was

on the terrestrial plant diversity, we excluded 13 algae and 36 aquatic plant taxa. Nine taxa were only present in samples that failed QC. Thus, our final dataset retained 288 terrestrial plant taxa detected in 316 samples.

We next explored the relationship between observed taxonomic richness and/or sample age against six measures of *sed*aDNA quality, with each measure calculated on a per sample basis.

MTQ and MAQ scores: Both scores correlate with richness when richness is low (<25-30; Fig. 3), which is likely an artifact of the requirement that the 10 best represented barcodes are required to calculate these scores. At higher richness values, both *MTQ* and *MAQ* scores are uniformly high. *MTQ* scores are minimally impacted by sample age (Figs. 3, S4A), although samples older than ~8.0 ka tend to have lowered *MAQ* scores (Fig. 3), which is driven by the Eaštorjávri South, Langfjordvannet, Kuutsjärvi, Nesservatnet, and, to a lesser extent, Jøkelvatnet records (Fig. S4B).

Raw read count summed across PCR replicates: Richness may be influenced by differences in total sequencing depth between samples, whereby we would expect increased total depth to correlate with richness as the likelihood of detecting read-rare taxa is increased (e.g. (*32*)). However, we do not observe a relationship between richness and raw read count (Fig. 3), suggesting that differences in sequencing depth do not influence richness in our data set. This is consistent with the results of the rarefied richness analyses (Table S2). We also do not observe a relationship between sample age and sequencing depth (Figs. 3, S4C), suggesting there is no temporal or stratigraphic bias in our ability to generate raw reads. We note that samples that passed or failed QC had comparable total sequencing depths.

Mean length of identified barcodes through time: As ancient DNA fragments into shorter molecules over time (*33*), a reduction in mean barcode length with sample age may suggest that longer barcodes are no longer preserved thus biasing estimates of temporal richness patterns. However, this assumes that barcode length is independent of taxonomic group and/or ecological community

composition, which may not always be the case. We do not observe a decrease in mean barcode length with age in samples that pass QC (Figs. 3, S4D). Samples that fail QC are often mean length outliers that show no relationship to age, but are rather an artifact of small sample sizes. Minor decreases in mean barcode length with sample age are observed for Kuutsjärvi and Langfjordvannet (Fig. S4D).

Mean proportion of weighted PCR replicates (wtRep): The mean *wtRep* provides a measure of mean taxon detectability in samples. If barcode template concentrations in *sed*aDNA extracts are low, then we would expect recovered richness to be limited, due to dropout, with a corresponding reduction in detectability of taxa that are observed. Consistent with this expectation, we find that mean *wtRep* values are comparable for samples with richness >25-30 (Fig. 3), but that mean *wtRep* and richness are correlated when richness is <25-30. However, we observe only a modest decrease in mean *wtRep* values with sample age (Fig. 3), suggesting that taxon detectability is not affected by age. The greatest age-related reductions in mean *wtRep* values are in samples from Langfjordvannet, Kuutsjärvi, Nesservatnet, and, to a lesser extent, Jøkelvatnet (Fig. S4E). We note, *a posteriori*, that mean *wtRep* and *MAQ* scores may not be independent measures, especially for samples with low richness (<25-30).

The proportion of raw reads assigned to terrestrial plant taxa: If there is co-amplification of non-terrestrial plant, algae, contaminant, and/or other off-target molecules, then terrestrial plant richness may be reduced by swamping. Interestingly, we observe that at least ~40% of reads are required to be identified as terrestrial plant taxa for observed richness to exceed ~60 taxa (Fig. 3). When richness is <60, we observe that the proportion of reads identified as terrestrial plant taxa decreases with richness (Fig. 3). However, we note that there is large variance around this trend and so, for example, samples from the Middle Holocene of Sandfjorddalen have comparable observed richness to Early Holocene samples from Gauptjern (Fig. S3), even though reads from the former are swamped by reads from aquatic plant taxa (Fig. S5). Across the entire data set, there is a gradual reduction in the proportion of reads identified as terrestrial plant taxa with sample age, which is driven by the

Eaštorjávri South, Kuutsjärvi, and Nesservatnet records (Figs. 3, S4F, S5). Samples that failed QC tended to have a lower proportion of reads identified as terrestrial plant taxa (Figs. 3, S4F, S5).

Overall, we found that the *MTQ* and *MAQ* score QC thresholds removed the worst performing samples. The records with the best *sed*aDNA quality are Gauptjern, Horntjernet, Nordvivatnet, Sandfjorddalen, and Sierravannet. Samples from the Early Holocene should be treated with more caution from the Eaštorjávri South, Kuutsjärvi, Langfjordvannet, and Jøkelvatnet records (Figs. S4, S5).

Local richness and species pool

To evaluate how richness and the local species pool changed through time, we calculated the accumulated and observed number of taxa in each sample within each lake as measures of local species pool and richness respectively. The local species pools increased over time for all catchments (Fig. 4) with the highest recorded at Jøkelvatnet (200 taxa), which today drains a catchment that has a Late Holocene glacier in its upper reaches (Fig. 1; Supplementary Materials, SI1). Rich species pools were also found at Gauptjern, which is at the border between pine and birch forest, and at Nordvivatnet and Langfjordvannet, which have a mixture of heathland, birch forest, and scree slope in their catchments. Somewhat lower species pools were found at the two sites in pine forest, Horntjernet and Kuutsjärvi, and at Sierravannet, a site with birch forest, and pine and larch plantations. The two shrub-tundra sites, Eaštorjávri South and Sandfjorddalen, had smaller species pools, similar to Nesservatnet, which is surrounded by heathland/mires (93 taxa) and located on the small island of Årøya.

There were clear differences among lakes, both in the overall levels of richness and in the change in richness over the period (Fig. 4). The mean (±SD) taxonomic richness (Hill N0) ranged from 20.6 (± 6.4) at Horntjernet to 65.5 (± 24.5) at Jøkelvatnet, whereas Hill N1 ranged from 14.9 (± 7.8) at Eaštorjávri South to 52.4 (± 20.5) at Jøkelvatnet (Fig. 4; Table S1). The rarefied richness based on read

count showed a strong correlation with observed taxonomic richness (R=0.82-0.99; Table S2), suggesting that the observed pattern was not affected by sequencing depth. The Hill N1 (common taxa) showed temporal patterns that mirrored those of observed taxonomic richness for all the lakes except Sierravannet (Fig. 4).

We observed a significant effect of the age of samples on taxonomic richness as indicated by statistically significant smooth terms in generalized additive mixed models (Table S3), except for Sierravannet, which only covered 2.6 ka, and where diversity suddenly dropped around 0.6 ka, corresponding to a putative flood event (Fig. S2). For two of the lakes, Eaštorjávri South and Nesservatnet, a near linear pattern of increase in taxonomic richness through time (edf=1) was recovered. On the other hand, Langfjordvannet had the most complex pattern of increase in richness (edf=5.93, Table S3). The steepest increase was seen in the Early and Middle Holocene for most lakes. Only at three sites, Nordvivatnet, Horntjernet and Gauptjern, did richness reach a plateau during the Late Holocene; for most lakes no levelling off was observed suggesting that richness is still increasing (Fig. 4).

Regional richness and species pool

To assess temporal patterns of regional species pool and richness, we calculated the accumulated number of detected taxa from the entire quality controlled data over the Holocene as a measure of the regional species pool, and the number of taxa detected in each sample as a measure of richness (Figs. 5A, S6). During the Early Holocene, there was a strong increase in the regional species pool size. The regional species pool increased monotonically from the Early Holocene to ca. 7.0 ka, the rate slowed in the period ca. 7.0-5.0 ka followed by an uptick from 5.0-3.3 ka before stabilising. The regional species pool levelled off over the last two millennia with an increase of just 10 taxa (3.5% of the total).

The mean (±SE) predicted taxonomic richness (Hill N0) based on a generalized additive model showed a steep increase during the Early Holocene from 13.8±3.9 to 31.8±1.5 taxa per sample when evaluated using 500-year time windows. Richness continued to increase during the Middle Holocene (33.4±1.5 to 42.7±1.3), and showed only a minor increase during the Late Holocene (43.7±1.3 to 45.9±2.0).

Richness in relation to local and regional species pools

To assess how local and regional species pool affects richness (beta-diversity) at respective scales, we used the accumulated number of taxa within a lake and 500-year time bin as measures of local and regional species pools respectively, and mean number of taxa at respective scales as richness estimates. There was a strong positive association between mean terrestrial plant richness and the local species pool of lakes, where 82% of the variation in local richness was explained by local species pool (R^2_{adj}=0.82, p<0.001, df=8; Fig. 6A). The mean richness of lakes represented about 24% to 37% taxa of the local species pool, except at Horntjernet, where richness represented only 18% taxa of the local species pool. The mean local richness increased by nearly four taxa (regression slope=0.36) for every 10 taxa that were added in the local species pool. Similarly, we found a strong positive correlation between mean richness per 500-year time period and total taxa available in the respective period, and 86% of the variation in richness was explained by the regional species pool (R^2_{adj}=0.86, p<0.001, df=21; Fig. 6B) where ~23% to 39% of the taxa from the regional species pool were represented by the mean richness. The mean regional richness increased by more than two taxa (regression slope=0.23) with the addition of 10 taxa in the regional species pool.

271 Impact of regional climate on plant richness

272 We used oxygen isotope ($\delta^{18}O$) values from the North Greenland Ice Core Project (NGRIP) (Andersen
273 *et al.*, 2004) as a proxy for temperature to assess the impact of regional climate on local richness during
274 different periods of the Holocene. Climate had a significantly positive effect on richness in the Early
275 Holocene (β=0.23, SE=0.05, $p<0.001$), a marginal negative effect in the Middle Holocene (β=-0.26,
276 SE=0.13, p=0.048), and a clear negative effect in the Late Holocene (β=-0.53, SE=0.12, $p<0.001$; Fig.
277 7A). In the Early and Late Holocene, temperature changed linearly through time at a rate (±SE) of 0.92
278 (±0.07) and -0.13 (±0.01) $\delta^{18}O$/ka respectively, whereas there was no directional change in temperature
279 across the Middle Holocene (Fig. 5B).

280

281 Effect of nutrient availability on plant richness

282 We used a new semi-quantitative nutrient index based on rock type and its weatherability to assess how
283 nutrient availability in the catchment area affects richness. We observed a positive correlation between
284 nutrient index and taxonomic richness for all three time periods (Fig. 7B) although this was not
285 significant for the Early Holocene (R^2_{adj}=0.36, F(1,6)=4.92, p=0.07), which also had the smallest
286 sample size. The nutrient index explained 51% and 35% of the variation in richness for the Middle
287 (R^2_{adj}=0.51, F(1,7)=9.22, p=0.02) and Late Holocene (R^2_{adj}=0.35, F(1,8)=5.92, p=0.04) respectively.
288 The nutrient-richness relationship was stronger for the Middle Holocene (β=0.21, SE=0.07, p=0.02)
289 than the Late Holocene (β=0.12, SE=0.05, p=0.04). The effect of nutrient index on taxonomic richness
290 was strongest when the impact of climate was negligible during the Middle Holocene. This suggests
291 that a significant cause of site-to-site variation and sub-regional richness patterns was soil nutrient
292 availability, which is dependent upon the bedrock and rate of weathering.

293

Discussion

The ability of *sed*aDNA to capture plant taxonomic richness

The mean observed taxonomic richness of terrestrial plants per sample and site (~21-66) is higher than that recovered for northern boreal sites based on pollen analyses (~20 taxa, *19*), but similar to pollen estimates from the Alps and Mediterranean (~30 taxa, *19*). The detected richness values are within the range that has been found in other recent studies of *sed*aDNA from northern sites (20-70 taxa per sample; *27*, *34*), although some shrub tundra (~13 per sample, *35*) and High Arctic (5-30 per sample, *36*) sites have notably lower estimates. Nevertheless, our results are consistent with other *sed*aDNA analyses that detect more taxa than pollen counts (*24*, *25*, *27*). Together with improved geographic fidelity due to a local signal, *sed*aDNA thereby improves our understanding of the spatial patterns and scale dependency of past plant diversity.

The temporal patterns evaluated here rely on the assumption that our ability to detect plant taxa in *sed*aDNA is not impacted by differential preservation, due to sample age or methodological problems such as DNA extract inhibition. Here we discarded samples of poor quality, that had metrics comparable to negative controls and thus may have been affected by methodological problems, and we broadly examined the quality of the retained samples. Half of our sites showed no evidence of declining *sed*aDNA quality with sample age, whereas the remainder had reduced quality in the Early Holocene interval. That our samples generally exhibited good *sed*aDNA quality throughout the study interval is likely due to a combination of excellent DNA preservation in the cold environments of high latitudes (*37*) and the young age of the samples (<11.7 ka) relative to the known upper limit of aDNA preservation (~560-780 ka, *38*). As multi-site *sed*aDNA studies become common, it will be crucial that data quality is scrutinized and, where possible, standardized to allow for biologically meaningful comparisons between sites.

Nutrient availability and plant richness

In considering the positive association between nutrient index and mean taxonomic richness of lakes for different periods of the Holocene, we highlight that our nutrient index is based on bedrock weathering, and the potential release of phosphorus, potassium, and calcium, which acts as a surrogate for alkalinity. During the Early Holocene, it is likely that nutrient release started immediately after deglaciation when liquid water was abundant (*39*) and light-demanding and disturbance-tolerant pioneer species could have survived on the nutrient-poor microhabitats, and thus showed weak overall association with the nutrient index. With continued warmer and possibly wetter conditions, leaching and nutrient release would have increased, thereby promoting richness in the Middle and Late Holocene. Relevant here is the fine spatial scale of the calcareous (alkaline) and siliceous (acidic) bedrock in northern Fennoscandia, with small and often linear, outcrops of metamorphic carbonate. This contrasts with the large calcareous limestone massifs found in younger geologies such as the European Alps, which have been shown to have effects on diversity over both short and long timescales (*11*). Given that there is also a positive association between nutrient index and total richness (representing a subset of the regional species pool), it is reasonable to consider nutrient index as an important driver for species pool development and hence regional richness (*40*). Indeed, it is the floristic variation between sites (beta-diversity) that accounts for the large difference between the local and regional species pools even today (*12*, *41*).

A steep Early Holocene increase in plant richness

The highest rate of increase in richness and in local and regional species pools is observed in the Early Holocene 11.7-8.3 ka. Due to their significant correlation, we cannot distinguish the effect of dispersal lags from temperature, and both factors likely contributed to the observed increase in diversity. Climate was also the driver for deglaciation, which increased the area available for colonisation. Three of our

342 records span a longer time period than examined here (Langfjordvannet: 16.7 ka, Nordvivatnet: 12.7
343 ka, Sandfjorddalen: 12.5 ka; Fig. S1F,H,I), and they, as well as macrofossils (14.5 ka, *42*) and pollen
344 records (13.9 ka, *43*) from other coastal sites in northern Fennoscandia, show that an Arctic pioneer
345 vegetation established towards the end of the Younger Dryas period (12.9-11.7 ka) and into the Early
346 Holocene. Thus, a species pool already existed at least along the coast at the start of our study period,
347 which is not the case for some of the inland sites (Gauptjern, Horntjernet, Kuutsjärvi) that were
348 deglaciated after the onset of the Holocene. Nevertheless, all sites exhibit a strong increase in richness
349 independent of location relative to deglaciation.

350 Especially during the rapid warming at 11.7-10 ka, we find a high increase in richness.
351 Additional factors other than climate and availability of land may have influenced richness in this
352 period. For example, biotic factors such as low levels of competition may have facilitated establishment
353 (*44*), and abiotic factors, particularly paraglacial processes, may have produced disturbance at the local
354 scale (*45*). On the other hand, dispersal lags may have limited richness and species pools, as for
355 example the 400-year time lag between climate and arrival of birch woodland which was estimated
356 based on plant macrofossils recovered from sediment cores (*46*). Nevertheless, the overall rapid
357 increase in diversity in an early phase of colonization is also recorded in pollen studies (*19*), and
358 expected given that they cover the development from pioneer to established vegetation communities.

359 Our richness patterns show a continued strong increase after ~11 ka, when the major expansion
360 of birch forest took place, and after ~10 ka when pine expanded into the region (*21*). Thus, in contrast
361 to the decrease in richness due to forest expansion observed in pollen studies (*13*, *19*), we found a
362 general increase in richness through time. This may be because *sed*aDNA analyses are less sensitive to
363 swamping by trees than pollen analyses and therefore better reflect habitat complexity (*25–27*).
364

365 Middle Holocene richness continues to increase

366 The moderate increase in local and regional species pools during the Middle Holocene (8.3-4.2 ka) was
367 marginally related to climate. The NGRIP record shows a temperature peak (end of the Holocene
368 Thermal Maximum) followed by slight cooling during this period. Richness levelled off in only two
369 lakes (Nordvivatnet and Sandfjorddalen) and one lake (Langfjordvannet) showed a hump in richness,
370 which we assume is due to local factors. For Gauptjern, palynological richness fluctuates around eight
371 taxa for this period (*47*), whereas our *sed*aDNA data show a clear increase. Pollen studies from
372 northern Fennoscandia have shown contrasting patterns through this period, including stable levels of
373 richness along a spruce-pine-birch tundra transect (*21*) and an overall increase in richness (*20*). The
374 closest sites previously studied for *sed*aDNA show stable richness at Varanger in Finnmark (*35*),
375 increasing richness in Svalbard (*36*), and fluctuating high richness in the Polar Urals (*34*). Seen from a
376 regional perspective, our richness curves are similar to those found in the temperate zone of Europe,
377 where a Middle Holocene richness increase is inferred to be due to human impact, but differ from those
378 of the boreal zone (*19*), probably due to lower influence of Holocene tree expansion in the *sed*aDNA
379 data. Thus, in contrast to many pollen studies, our *sed*aDNA data show an increase in richness and
380 species pool for the Middle Holocene. As the climate was relatively stable during this period, we
381 speculate that the increase in richness may have been mostly driven by dispersal lags, resulting in
382 delayed establishment of some taxa in the region, and/or early habitat diversification allowing for a
383 greater variety of niches, including the development of heathland, meadows, and mires (*14*).
384
385 Late Holocene richness nears a plateau
386 The regional species pool clearly levelled off during the past few millennia suggesting that a near
387 saturation point was reached. The slight cooling and well-known instability in this period (*48*)
388 negatively impacted richness, potentially as a consequence of the cooling-induced withdrawal of the

389 forest in the region (*14*, *21*). Palynological richness in northern Fennoscandia also increases slightly
390 (*47*) or is variable (*21*) during this period. Richness also increases at sites in the boreal and temperate
391 regions of Europe, mainly due to human land use impacts (*19*, *22*). The reason for levelling off at the
392 regional scale in northern Fennoscandia is likely due to the near-saturation of the regional species pool
393 and the overall low impact of human land use within the catchments.

394 In contrast to the regional scale, our data suggest that the local species pools and richness are
395 not yet saturated. This is in contrast to what has been observed in studies of modern vegetation, where
396 there appears to be no effect of time since glaciation for local (plot level) richness, whereas a legacy of
397 the ice age is inferred for richness at the pan-Arctic (floristic region) scale (*16*). This apparent
398 contradiction may be the result of scale and environmental spatial variation. Our catchments are larger
399 than the plots studied by Stewart et al. (*16*), and therefore allow for co-existence of different vegetation
400 types. Soils develop slowly on hard felsic and mafic rocks and have low buffering capacity resulting in
401 nutrient loss and the partial development of oligotrophic vegetation types such as acid heaths and
402 ombrotrophic mires. These have their own floras and some species are restricted to these environments.
403 Indeed, mires and heath vegetation expanded in the region during the Late Holocene (*14*, *21*).
404 Depending upon the local bedrock, a given area may thus gradually come to include additional
405 vegetation types, allowing more hardy species to grow and total richness to increase while retaining the
406 more demanding species in more favourable areas of the catchment. In addition, infilling of the lake
407 creates wetland zones that also may include terrestrial taxa. Thus, a continued increase in richness and
408 local species pools may be due to habitat diversification.
409

410 Conclusions

411 We are aware that our study has several limitations. First, one should be aware that *sed*aDNA analyses
412 based on p6-loop metabarcoding has taxonomic biases, as some species-rich families such as

Salicaceae, Poaceae and Cyperaceae are poorly resolved due to haplotype sharing (*30*, *49*). We have used a local reference database to maximise taxonomic resolution and note that this is also an issue for traditional palynological proxies. Second, we acknowledge that the initial steep increase for our species pool estimates at the start of the Holocene constitute a sampling probability artifact, as plant taxa are known from the region in the late glacial (*42*, *43*). However, we note that a consistent steep increase continues throughout the Early Holocene interval, which we do not consider to be a sampling artifact. Third, we assume that the NGRIP record is representative of the climate of northern Fennoscandia. This record is in accordance with reconstructions of local climate in northernmost Fennoscandia based on macrofossils and pollen, although local variation does exist especially due to the proximity of the Norwegian Coastal Current, which is an extension of the Atlantic Gulf Stream (*43*). Lastly, we have not considered human impact as a potential driver of richness or species pools, but emphasise that this is considered to have been low in northern Fennoscandia as compared to other regions in Europe (*14*).

We present terrestrial plant richness and species pools inferred from 10 Holocene *sed*aDNA records covering environmental gradients in northern Fennoscandia. Our development of new quality control metrics to standardize data, together with improved taxonomic precision and known source areas (hydrological catchments of the lakes) allows for meaningful estimates of taxonomic richness, its spatial variation, and temporal trends, which show a unique increasing pattern of terrestrial plant richness over the Holocene. Our data reveal a steep increase in diversity in the Early Holocene related to the concurrent increase in temperature at that time and abundant vacant niches. However, the richness and the local and regional species pools continued to increase through the Middle and Late Holocene, although at a slower rate, suggesting that dispersal lags and habitat diversification had a major impact on diversity in these latter periods. In addition, we found that local nutrient levels, calculated based on bedrock type, had a strong impact on the overall levels of richness. Individual differences were observed among our sites, but our novel combined and standardized *sed*aDNA

analyses of 10 sites provides a superior representation of the overall regional patterns in plant taxonomic richness over the Holocene as compared to traditional approaches. We suggest that plant diversity will continue to, and perhaps markedly, increase in northern Fennoscandia as a consequence of the northward movement of warm adapted species due to ongoing climate warming (sensu *1*). Expanding human impacts, including niche construction and introductions, within the region would further increase diversity. However, increases in diversity may be tempered by dispersal lags and the time taken for habitats to diversify as is suggested by our Holocene data set.

Integration of long-term paleo- and contemporary ecological data will be key to understanding, predicting, and managing the consequences of ongoing climate warming in northern ecosystems. Our study showcases how regional scale *sed*aDNA data can provide refined paleoecological insights into richness and species pools, as compared to traditional proxies, which will increase the precision of integrative ecological models.

Materials and Methods

Study area, site selection, and properties

The study area covers northernmost Fennoscandia above the Arctic Circle (at 67.75-70.43 N and 19.62-30.02 E) with nine lakes in Norway and one in Finland (Fig. 1, Data set S1). Site climatic and environmental properties are given below, whereas geology and vegetation descriptions are in the Supplementary Materials, SI1 and SI2.

Site selection. We selected 10 sites with the aim of minimising variation in environmental and potentially taphonomic variables (such as lake size and altitude), whilst covering the variation of biogeographical variables and particularly intra-regional climate. All sites are therefore small to medium sized lakes, with small catchments, no or minimal input streams, and a location above the maximum marine limit. We aimed to cover the major vegetation types in the region including the

northernmost spruce and pine forest, the more widespread birch forest as well as subarctic grassland below the present-day treeline (Data set S1).

Climate. The Norwegian sites are located in the three most northerly Norwegian temperature regions (TR4-TR6) and precipitation regions (RR11-RR13), as defined by Hansen-Bauer and Nordli (*50*). Statistical analysis has established that these are the most homogenous sub-regions related to common drivers of regional forcing, particularly sea-level pressure over the North Atlantic and North Atlantic Oscillation (NAO) (*51*). The Finnish site (Kuutsjärvi) is close to the easternmost part of Norway, with a similar continental climate.

Environment. The site environmental data was taken from published sources: site altitude, lake area, catchment area and climatic variables was generated from the NAVINA-NVE online tools (https://www.nve.no/karttjenester/) and catchment geology from the Geological Survey of Norway (NGU) online mapping system (https://www.ngu.no/en). Given that the role of parent material is particularly important for plant growth in both sub-arctic and Alpine environments (*52*) it was deemed potentially valuable to classify the sites by the geologically derived nutrient resource environment (see Equation 2). In most cases values from the bedrocks of the sites are not available so typical values measured from a suite of rocks from the Caledonian-nappe metamorphic rocks from north Troms was used (*12*) the values of which can be found in Data set S1. However, in the case of Nordvivatnet and Sandfjorddalen values could be taken from studies of the alteration of Neoproterozoic tillites of the Varanger region (*53*). The major methodological uncertainties with such an index is the role of both the moraine cover and the development of a soil organic matter store. The moraine cover is typically pre-weathered to some extent and probably reduces the effect of the local bedrock. This approach is appropriate for the geologically mediated plant nutrients and nutrient storage and cycling governed by the development of a soil organic matter (SOM) store.

485 Fieldwork and lake sediment coring

486 We collected cores from seven of the ten lakes from northern Fennoscandia between February and
487 April 2017 (Fig. 1; Data set S1), whereas cores from three lakes were obtained from previous studies
488 (see below). For each of six of the lakes, we retrieved sediment in a single 10-cm diameter polyvinyl
489 chloride (PVC) pipe, using a modified Nesje piston-corer (*54*) from the deepest and generally central
490 part of the lake. At Lake Gauptjern, two Nesje cores were retrieved (EG03, EG13). We monitored for
491 potential cross contamination using a DNA tracer mixed into Vaseline, which we applied to the piston
492 immediately prior to coring. This tracer consisted of DNA extracted from a non-native plant, the
493 Christmas cactus (*Schlumbergera truncata*) (see Supplementary Materials, SI3). After coring, we cut
494 the pipe into 1.0-1.2 m long sections in the field and immediately sealed the ends to minimize
495 contamination from modern environmental DNA (eDNA). For six of the lakes, we collected up to 1-m
496 long cores using a 4-cm diameter rod-operated Multisampler (Eijkelkamp 12.42; Giesbeek, The
497 Netherlands), which usually captured the water-sediment interface (Data set S2). At Sandfjorddalen,
498 two sequential Multisampler cores were taken from the same hole, resulting in a 149 cm core. All core
499 sections were kept cold during transport to and storage in a dedicated cold room (4 °C). During storage,
500 water from the majority of the Multisampler cores leaked out, which resulted in shrinkage of these
501 cores.
502
503 Core sampling
504 The Nesje cores were split longitudinally, with one half used for destructive analyses (loss-on-ignition,
505 LOI; *sed*aDNA) and the other for high-resolution imagery. Sampling for destructive analyses was
506 conducted in the dedicated ancient DNA laboratory facility at The Arctic University Museum of
507 Norway (TMU), using sterile implements. We sampled all cores starting at the base and fully cleaned
508 the laboratory between sampling cores from different lakes. At each selected 1-cm layer, we first

509 removed and discarded the top ~2 mm of exposed sediment surface. We then removed a further ~3 mm
510 (~5-10 g) of the underlying sediment surface, which we retained for LOI analysis. Finally, we then
511 sampled ~10-20 g of the remaining underlying sediment for *sed*aDNA analysis, taking care not to
512 sample sediment immediately adjacent to the PVC pipe. To detect contamination from exogenous
513 sources of environmental DNA, we took sampling negative controls that consisted of 100 µL of
514 exposed molecular biology grade water.

515 For the Multisampler cores with remaining water and highly liquid surface sediment, we first
516 siphoned off and discarded the water. We then siphoned and retained the liquid surface sediment at 1
517 cm intervals. For the remaining sediment, and for Multisampler cores that had shrunk due to water loss,
518 we extruded the cores at 1 cm intervals, starting at the base of the core. At each interval, the outer ~5
519 mm of sediment was removed and retained for LOI analysis. The remaining ~3 cm diameter sediment
520 was retained for *sed*aDNA analysis. Sampling conditions and controls were as described above.

521 We sampled sediment from three cores that had been previously collected and were available to
522 us. These consisted of records from Langfjordvannet (*31*), Jøkelvatnet (*55*), and Kuutsjärvi (*56*). For
523 the Langfjordvannet and Jøkelvatnet cores, sampling was conducted within the clean labs of
524 GeoMicrobiology at the Department of Earth Science, University of Bergen, Norway following the
525 approach mentioned above. Sampling of the Kuutsjärvi core was conducted in the Physical Geography
526 department at Stockholm University, Sweden using sterilized tools and with all surfaces cleaned with
527 bleach. We took negative sampling controls at both institutions as described above.

528

529 Core photography and loss-on-ignition analyses

530 The intact core halves were photographed at high resolution using a Jai L-107CC 3 CCD RGB Line
531 Scan Camera mounted to an Avaatech XRF core scanner at the Department of Geosciences, The Arctic
532 University of Norway in Tromsø. We calculated mass LOI, by first drying samples 105 °C overnight

and then igniting the sample at 550 °C for 2 hours. We report the percentage of dry mass lost after ignition (*57*). LOI data and high resolution core scanning imagery are presented in Data set S3 and Fig. S1.

Composite core construction and age-depth modelling

We opportunistically collected macrofossils for radiocarbon (^{14}C) dating during sampling for LOI and *sed*aDNA, where possible. If additional macrofossils were required, we sieved sediment to concentrate macroscopic plant remains suitable for dating. Two sieves of 500 and 250 µm were stacked while sieving to catch plant macrofossil remains. Ultrapure water from the Milli-Q system was used for sieving and cleaning, and samples were kept cool in Eppendorf tubes with water before shipping for dating. We photographed and identified all macrofossils prior to their destruction during radiocarbon dating. Samples were radiocarbon dated using Accelerator Mass Spectrometry (AMS) at the Poznań Radiocarbon Laboratory of the Adam Mickiewicz University, Poland (*58*) (Data set S3).

For multiple-core records from the same site, we aligned cores based on combinations of LOI values, visible stratigraphy, and/or radiocarbon dates to create composite core records (Fig. S1; Data sets S2, S3). For Gauptjern, we used the LOI profile and radiocarbon dates produced by Jensen & Vorren (*47*) to guide composite age-depth model construction (Fig. S1B; Data set S3). All reported depths are based on the composite cores and begin at the water-sediment interface, which was determined either by its successful capture, field notes, or previously published information (Data set S2). We note that the composite depths reported here differ for two of three previously published records (*31*, *47*, *55*) (Data set S3). For Langfjordvannet, we increased depths by 26 cm to account for the amount of sediment reported missing from the top (*31*), whereas for Gauptjern, we removed 340 cm (water depth) and adjusted remaining depths for differing deposition rates among all cores, due to an uneven bedrock surface (*47*).

We constructed Bayesian age-depth models using *bacon* v.2.3.4 (*59*) in R v3.4.4 (*60*), using the IntCal13 calibration curve (*61*). Each basal modeled age was ≤2 cm below the basal radiocarbon date, with the exception of Langfjordvannet where the basal radiocarbon date falls within a slump that extends to the base of the core. We were unable to confidently model the basal 31 cm of Jøkelvatnet and 22 cm of Kuutsjärvi, as extrapolated ages were highly influenced by accumulation rate priors. We fixed the top of each record to zero, based on the composite cores beginning at the water-sediment interface. The default section thickness of 5 cm was used for all age-depth models, with the exception of Sandfjorddalen, which shrank from the 149 cm collected to 92 cm analyzed. We therefore selected a 2 cm thickness for the Sandfjorddalen age-depth model. We excluded two dates (Poz-108675, Poz-108983) from the Sierravannet age-depth model that occurred in a putative flood layer (Fig. S1J).

Sedimentary ancient DNA data generation

We performed all pre-PCR steps at the dedicated ancient DNA facilities at TMU, which are in a separate building to post-PCR facilities. We homogenized Holocene-aged DNA samples by holding samples on a pulse vortexer for ~1 min. We extracted DNA from 0.25-0.35 g of sediment (Data set S4) using a modified form of the Qiagen DNeasy PowerSoil PowerLyzer (Qiagen Norge, Oslo, Norway) protocol, following the Zimmermann *et al*. (*62*) protocol, as modified by Alsos *et al*. (*63*). We included one negative extraction control, consisting of no input, for every 10 sediment extractions. We also extracted DNA from 10 samples using the protocol 15 of Heintzman *et al*. (in prep) and six samples using the carbonate protocol of Capo *et al*. (submitted).

We amplified DNA and control extracts using 'gh' primers (*64*) that target the vascular plant trnL p6-loop locus of the chloroplast genome (Data set S5). The gh primers were unique dual-tagged with an 8 or 9 base pair tag, modified from Taberlet et al. (*65*). We used differing tag lengths to ensure that nucleotide complexity was maintained during amplicon sequencing runs. A total of eight PCR

581 replicates were amplified per extract. We included negative PCR controls, consisting of water as input,
582 to monitor for contamination during the PCR. We additionally included negative and positive PCR
583 controls in the post-PCR lab, the latter of which consisted of one of six synthetic sequences (available
584 at https://github.com/pheintzman/metabarcoding) (see also Supplementary Materials, SI4). These post-
585 PCR lab controls were added to wells without disturbing other sealed sample and control wells and
586 were used to monitor PCR reaction success. However, they are not comparable to other negative
587 controls and samples, due to exposure to the post-PCR lab atmosphere, and so they were excluded from
588 further analysis. We checked for successful amplification using gel electrophoresis (2% agarose).
589 We pooled up to 384 PCR products (the maximum number of available tags) and then cleaned
590 the resulting pool following Clarke *et al*. (*35*). Each amplicon pool was then converted into a DNA
591 library at either Tromsø or FASTERIS, SA (Switzerland). The Tromsø protocol used the Illumina
592 TruSeq DNA PCR-free protocol (Illumina, Inc, CA, USA) with unique dual-indexes, except that the
593 magnetic bead cleanup steps were modified to retain short amplicons, whereas FASTERIS used the
594 PCR-free MetaFast protocol to produce single-indexed libraries following Clarke *et al*. (*35*). Each
595 library was sequenced on ~10% of 2x 150 cycle mid-output flow cells on the Illumina NextSeq
596 platform at either FASTERIS or the Genomics Support Centre Tromsø (GSCT) at The Arctic
597 University of Norway in Tromsø, or on 50% of a 2x 150 cycle flow cell on the Illumina MiSeq
598 platform at FASTERIS. Full sample preparation metadata is provided in Data set S5.
599
600 Bioinformatics
601 We followed a bioinformatics pipeline that uses a combination of the ObiTools software package (*66*)
602 and custom R scripts (available at https://github.com/Y-Lammers/MergeAndFilter). Briefly, we merged
603 and adapter-trimmed the paired-end reads with SeqPrep (https://github.com/jstjohn/SeqPrep/releases,
604 v1.2). We then demultiplexed the merged data using an 8 bp tag-PCR replicate lookup identifier

(provided in Data set S5), which ignored the non-informative terminal base for 9 bp tags, and collapsed identical sequences. We removed putative artifactual sequences from our data, which may have derived from Illumina library index-swaps or PCR/sequencing errors. For each PCR replicate, we removed sequences represented by ≤2 reads. We next identified barcode sequences that had 100% identity agreement with a local taxonomic reference database (*ArctBorBryo*) containing 2445 sequences of 815 arctic and 835 boreal vascular plants, as well as 455 bryophytes (*30*, *49*, *67*). In addition, we matched our data set to the *EMBL* (rl133) nucleotide reference database. We separately compared our barcode data set against the barcode sequence of the DNA tracer, with the closest match consisting of 85% identity (see Supplementary Materials, SI3). We therefore consider the DNA tracer not to be present in our data set. We further removed identified sequences that 100% matched against two *blacklists* (https://github.com/Y-Lammers/Metabarcoding_Blacklists) consisting of either synthetic sequences (n=6), sequences that represented homopolymer variants of a more read-dominant sequence, a potential random match, or food contaminants (n=111) (Data set S6). We further removed any sequences represented by fewer than 10 reads and/or three PCR replicates within the entire data set, as well as 61 low-frequency sequences that were only retained by analysis of the entire data set but removed if analyses were conducted on a per-lake basis (Data set S6). If multiple sequences were assigned to the same taxon, then the data were merged using the sum of all assigned reads and the maximum number of PCR replicates (Data set S7). The final taxonomic assignment of the retained sequences was determined using regional botanical taxonomic expertise by Alsos and following the taxonomy of the Panarctic Flora (*68*) and Lid's Norsk Flora (*69*). We identified two species of *Vaccinium* based on a poly-A region at the 3' end of the p6-loop locus. If there were ≤5 or >8 As, then barcodes were respectively assigned to *V. myrtillus* or *V. vitis-idaea*. We further excluded barcodes that were identified above the family level based on alignment to the local reference database, *ArctBorBryo*. Among the identified plant taxa, only terrestrial vascular plants and bryophytes were retained for all

629 downstream analyses (Data set S6). We only included Holocene-aged (11,700 ka to present) samples
630 for downstream analysis. We note that we use the term taxonomic richness to include taxa identified to
631 various ranks from the species to family levels.
632
633 Assessment of sedimentary ancient DNA data quality
634 Our *MTQ* and *MAQ* score thresholds excluded all negative controls, which had an *MTQ* of <0.75 and
635 *MAQ* of <0.1. Across our entire data set, 16 samples were extracted more than once. We included data
636 from the DNA extract that yielded the greatest *MAQ* score. In three cases with equal *MAQ* scores, we
637 selected replicate one for inclusion (Data set S4).
638 After data filtering, we found that there was often large variation in the counts of retained reads
639 between PCR replicates within a sample (from hundreds to tens of thousands). Although read-dominant
640 barcodes are likely to be detected in all PCR replicates, there is likely to be dropout of other barcodes
641 in replicates with lower counts of retained reads. In contrast, rare barcodes are more likely to be
642 detected in replicates with high retained read counts. We therefore developed a barcode detectability
643 measure - *wtRep* - to account for differences in relative counts of retained reads, by weighting PCR
644 replicates based on retained read count relative to the total retained read count across all PCR
645 replicates, on a per sample basis (see Equation 3). For example, if a barcode were detected in replicates
646 one and three, but undetected in the remaining six replicates, the *wtRep* would as shown in Equation 1.
647
648 Equation 1. Example definition of *wtRep*.

$$wtRep = \frac{retained\ read\ count(rep.1) + retained\ read\ count(rep.3)}{\Sigma\ retained\ read\ count(reps.1-8)}$$

649
650 If a PCR replicate were not represented in the retained read data, then it would not contribute to the
651 *wtRep* score. A limitation of the *wtRep* score is that it will overrepresent detections in samples or

652 negative controls with few barcodes and/or detections. For this reason, we only applied *wtRep* for a
653 sample if the average proportion of replicates across the sample was ≥0.33 and there were ≥10
654 barcodes present after filtering. For samples that failed this threshold, we used a standard proportion of
655 PCR replicates as a measure of detectability (e.g. 0.25 for the above example).

656 We further explored the quality of our *sed*aDNA data by examining four measures. For each
657 sample, we calculated the (1) total count of raw reads (summed across PCR replicates), (2) mean
658 barcode length (in base pairs, bp) across all retained barcodes, (3) mean proportion of weighted PCR
659 replicates (*wtRep*; see above) across all final barcodes, and (4) proportion of raw reads assigned to
660 terrestrial plant taxa. We compared each of these four measures to both observed taxonomic richness
661 (Hill-N0) and/or time.

662

663 Numerical and statistical analyses

664 Using the proportion of weighted PCR replicates (*wtRep*), we measured taxonomic richness (diversity)
665 based on Hill numbers (N0 and N1) (*70*), as they are easily interpretable and provide information on
666 both the rare and common taxa within a community (*13*). Hill numbers have been widely used as
667 common metrics to link different ecological attributes (*71*) as well as increasingly used in DNA-based
668 diversity analyses (*72*). For each sample, we calculated taxonomic richness as Hill N0 (total number of
669 observed taxa), and number of abundant taxa as Hill N1 (see Equation 2), which is the exponent of the
670 Shannon index (*13*). To evaluate if the disproportionate sequencing depth has affected the taxonomic
671 richness estimates, we also calculated rarefied taxonomic richness based on the lowest number of reads
672 assigned to a sample within a lake. We calculated Pearson's product-moment correlation between
673 rearefied and observed (Hill N0) taxonomic richness to evaluate the correspondence between
674 approaches (Table S2).

675

676 Equation 2. Definition of Hill N1.

$$Hill\ N1\ =\ exp\ (-\sum plogp)$$

677 Where p_i is the proportion of each species within a sample.

678

679 We used generalized additive models (GAMs) (*73*) to evaluate temporal biodiversity changes
680 during the Holocene. GAMs are very efficient at uncovering nonlinear covariate effects (*74*) and
681 handling non-normal data that are typical in palaeoecology (*75*). We treated Hill N0 and N1 as the
682 response, and median calibrated age of the samples as predictor variables, and used the "poisson"
683 family with log link. The Hill N1 was rounded to the nearest whole number prior to GAM analysis. To
684 account for residual temporal autocorrelation between samples, we also included a continuous time
685 first-order autoregressive process (CAR(1)) in generalized additive mixed models (GAMM; (*75*)). For
686 both GAM and GAMM models, the fitted lines are based on the predicted values for 300 points
687 covering the entire range of sample age for each lake. We used a critical value from the t distribution to
688 generate a pointwise 95% confidence interval (*75*). We found near identical results for taxonomic
689 richness between GAM and GAMM models (Fig. S7; Table S3). In the cases of two shorter cores from
690 Nesservatnet and Sierrvatnet, the GAMM provided a reasonable fit to the data, and hence was included
691 in the main results.

692 We also evaluated how the local and regional species pools affected richness estimates at
693 respective scales. We define the local and regional species pool as the cumulative number of taxa
694 recorded within a lake or the total region, respectively. First, we calculated the cumulative number of
695 detected taxa from the oldest to the youngest samples across all lakes as an indicator of the
696 development of the regional species pool, and compared that qualitatively to the taxonomic richness of
697 all samples through time. In addition, we generated a regional species pool of total species recorded
698 within each 500-year time bin. We extracted major trends of richness based on 500-year bins using

699 GAM for the Early-, Middle-, and Late Holocene. We also used GAM to highlight the regional trend in
700 taxonomic richness through time. Then, we performed linear regression by considering the mean
701 number of taxa within a lake, and within a 500-year time bin as the response variables, and the
702 respective species pools as the predictor variables to test whether observed richness is correlated to the
703 species pools of respective scales.

704 To examine the relationship of climate and diversity estimates, we used oxygen isotope ($\delta^{18}O$)
705 values from the North Greenland Ice Core Project (NGRIP) (Andersen *et al.*, 2004) as a proxy for
706 temperature. This has limitations as a regional record for northern Fennoscandia because of geographic
707 distance, but its advantage is that it is independent of vegetation-based reconstructions and it covers the
708 whole period of interest. It shows similar trends in annual temperature as both proxy-based and
709 simulated reconstructions for the northern North Atlantic region (Marsicek *et al.*, 2018). Because
710 summer temperature and growing degree days (GDD) are strong drivers of vegetation response to
711 climate in the north, we note that Holocene GDD sums probably remained higher than present through
712 much of the Holocene, as patterns of both seasonality and season length changed (Marsicek *et al.*,
713 2018). The Early Holocene temperature change was steeper than the Middle- and Late Holocene, and
714 we expect the richness pattern to differ among those periods. Thus, we assigned $\delta^{18}O$ data of 50 years
715 resolution to the nearest age estimate of samples, and split diversity estimates and $\delta^{18}O$ values into
716 three periods (Early:11.7-8.3 ka, Middle: 8.3-4.25 ka, and Late Holocene: 4.25-0.0 ka) following
717 Walker *et al*. (*76*). To evaluate how changes in temperature affected the richness pattern of the different
718 Holocene periods, we compared regression slopes of the Middle and the Late Holocene to the Early
719 Holocene using a linear mixed model with taxonomic richness as the response and an interaction
720 between $\delta^{18}O$ and the Holocene period as predictor along with lakes as the random variable.

721 We used a new semi-quantitative nutrient index derived from the sum of the phosphorus (P),
722 potassium (K), and calcium (Ca) content of the rocks modified by a measure of weatherability, in this

723 case the extended Moh's hardness of the least resistant major mineral in the rock type (H_{min}) (see
724 Equation 3). The natural logarithm of Ca content was used as this has been shown to have a strong
725 relationship with pH, which is critical to the availability of nutrients especially P (*12*). We performed
726 linear regression treating mean taxonomic richness of different periods of the Holocene as the response
727 and nutrient index as the predictor. The richness data were log transformed while evaluating the impact
728 of temperature and nutrients.
729
730 Equation 3. Definition of Nutrient Index.

$$Nutrient\ index\ (NI) = \frac{(P + K + ln(Ca))}{H_{min}}$$

731 Where P, K and Ca are total phosphorus, potassium and calcium in ppm, and H_{min} the hardness of the
732 most easily weathered principal mineral in the local bedrock.
733
734 Unless otherwise stated, all the analyses were performed using the *vegan* package (*77*) in R and
735 base *R (60)*. The library *mgcv* (*73*) was used for GAM model building. All plots were created using
736 *ggplot2* (*78*).
737

738 **Supplementary Materials**

739 Supplementary Information 1. Site geology.
740 Supplementary Information 2. Site vegetation.
741 Supplementary Information 3. DNA tracer.
742 Supplementary Information 4. Positive control synthetic sequences.
743 Fig. S1. Alignments of core LOI, high-res. imagery, and Bayesian age-depth models.
744 Fig. S2. A potential flood event does not impact the Sierravannet diversity trend.

745 Fig. S3. Observed taxonomic richness in each sample by lake and time including samples not passing
746 quality controls.
747 Fig. S4. Six measures of *sed*aDNA data quality by lake and time.
748 Fig. S5. The assignments of reads processed by the bioinformatic pipeline.
749 Fig. S6. The accumulated regional species pool and taxonomic richness of each sample across the
750 Holocene of northern Fennoscandia excluding two temporally-short records from Nesservatnet (EG02)
751 and Sierravannet (EG07).
752 Fig. S7. Comparison between GAM and GAMM(CAR(1)) models of taxonomic richness through time.
753 Table S1. Summary of all data used or generated in this study.
754 Table S2. Correlations between observed and rarefied taxonomic richness for each lake.
755 Table S3. Summary of generalized additive models (GAMs), and generalized additive mixed models
756 (GAMMs) with a continuous time first-order autoregressive (CAR(1)) process.
757 Data set S1. Geographic and site metadata for the ten lakes.
758 Data set S2. Composite core construction and Bayesian age-depth modelling.
759 Data set S3. Sample metadata, including depths, LOI values, dates, and modelled ages.
760 Data set S4. Full sample metadata including QC and bioinformatic sequence processing.
761 Data set S5. Primer tag to sample lookup, library preparation, and sequence accession data.
762 Data set S6. List of all identified barcodes, including those blacklisted, and their taxonomic
763 assignments and functional groups.
764 Data set S7. Read counts and PCR replicate detections for all retained taxa across all samples.

765 **References**

766 1. S. Harrison, Plant community diversity will decline more than increase under climatic warming.
767 *Philos. Trans. R. Soc. Lond. B Biol. Sci.* **375**, 20190106 (2020).

768 2. A. J. Suggitt, D. G. Lister, C. D. Thomas, Widespread effects of climate change on local plant
769 diversity. *Curr. Biol.* **29**, 2905–2911.e2 (2019).

770 3. F. Pilotto, I. Kühn, R. Adrian, R. Alber, A. Alignier, C. Andrews, J. Bäck, L. Barbaro, D.
771 Beaumont, N. Beenaerts, S. Benham, D. S. Boukal, V. Bretagnolle, E. Camatti, R. Canullo, P. G.
772 Cardoso, B. J. Ens, G. Everaert, V. Evtimova, H. Feuchtmayr, R. García-González, D. Gómez
773 García, U. Grandin, J. M. Gutowski, L. Hadar, L. Halada, M. Halassy, H. Hummel, K.-L.
774 Huttunen, B. Jaroszewicz, T. C. Jensen, H. Kalivoda, I. K. Schmidt, I. Kröncke, R. Leinonen, F.
775 Martinho, H. Meesenburg, J. Meyer, S. Minerbi, D. Monteith, B. P. Nikolov, D. Oro, D. Ozoliņš,
776 B. M. Padedda, D. Pallett, M. Pansera, M. Â. Pardal, B. Petriccione, T. Pipan, J. Pöyry, S. M.
777 Schäfer, M. Schaub, S. C. Schneider, A. Skuja, K. Soetaert, G. Spriņģe, R. Stanchev, J. A.
778 Stockan, S. Stoll, L. Sundqvist, A. Thimonier, G. Van Hoey, G. Van Ryckegem, M. E. Visser, S.
779 Vorhauser, P. Haase, Meta-analysis of multidecadal biodiversity trends in Europe. *Nat. Commun.*
780 **11**, 3486 (2020).

781 4. M. Zobel, The species pool concept as a framework for studying patterns of plant diversity. *J. Veg.*
782 *Sci.* **27**, 8–18 (2016).

783 5. J.-P. Lessard, J. Belmaker, J. A. Myers, J. M. Chase, C. Rahbek, Inferring local ecological
784 processes amid species pool influences. *Trends Ecol. Evol.* **27**, 600–607 (2012).

785 6. A. D. Bjorkman, I. H. Myers-Smith, S. C. Elmendorf, S. Normand, N. Rüger, P. S. A. Beck, A.
786 Blach-Overgaard, D. Blok, J. H. C. Cornelissen, B. C. Forbes, D. Georges, S. J. Goetz, K. C.

Guay, G. H. R. Henry, J. HilleRisLambers, R. D. Hollister, D. N. Karger, J. Kattge, P. Manning, J. S. Prevéy, C. Rixen, G. Schaepman-Strub, H. J. D. Thomas, M. Vellend, M. Wilmking, S. Wipf, M. Carbognani, L. Hermanutz, E. Lévesque, U. Molau, A. Petraglia, N. A. Soudzilovskaia, M. J. Spasojevic, M. Tomaselli, T. Vowles, J. M. Alatalo, H. D. Alexander, A. Anadon-Rosell, S. Angers-Blondin, M. te Beest, L. Berner, R. G. Björk, A. Buchwal, A. Buras, K. Christie, E. J. Cooper, S. Dullinger, B. Elberling, A. Eskelinen, E. R. Frei, O. Grau, P. Grogan, M. Hallinger, K. A. Harper, M. M. P. D. Heijmans, J. Hudson, K. Hülber, M. Iturrate-Garcia, C. M. Iversen, F. Jaroszynska, J. F. Johnstone, R. H. Jørgensen, E. Kaarlejärvi, R. Klady, S. Kuleza, A. Kulonen, L. J. Lamarque, T. Lantz, C. J. Little, J. D. M. Speed, A. Michelsen, A. Milbau, J. Nabe-Nielsen, S. S. Nielsen, J. M. Ninot, S. F. Oberbauer, J. Olofsson, V. G. Onipchenko, S. B. Rumpf, P. Semenchuk, R. Shetti, L. S. Collier, L. E. Street, K. N. Suding, K. D. Tape, A. Trant, U. A. Treier, J.-P. Tremblay, M. Tremblay, S. Venn, S. Weijers, T. Zamin, N. Boulanger-Lapointe, W. A. Gould, D. S. Hik, A. Hofgaard, I. S. Jónsdóttir, J. Jorgenson, J. Klein, B. Magnusson, C. Tweedie, P. A. Wookey, M. Bahn, B. Blonder, P. M. van Bodegom, B. Bond-Lamberty, G. Campetella, B. E. L. Cerabolini, F. S. Chapin, W. K. Cornwell, J. Craine, M. Dainese, F. T. de Vries, S. Díaz, B. J. Enquist, W. Green, R. Milla, Ü. Niinemets, Y. Onoda, J. C. Ordoñez, W. A. Ozinga, J. Penuelas, H. Poorter, P. Poschlod, P. B. Reich, B. Sandel, B. Schamp, S. Sheremetev, E. Weiher, Plant functional trait change across a warming tundra biome. *Nature*. **562**, 57–62 (2018).

7. A. K. J. Niskanen, P. Niittynen, J. Aalto, H. Väre, M. Luoto, Lost at high latitudes: Arctic and endemic plants under threat as climate warms. *Divers. Distrib.* **25**, 809–821 (2019).

8. J. Lenoir, R. Bertrand, L. Comte, L. Bourgeaud, T. Hattab, J. Murienne, G. Grenouillet, Species better track climate warming in the oceans than on land. *Nature Ecology & Evolution*. **4**, 1044–1059 (2020).

9. C. M. Hulshof, M. J. Spasojevic, The edaphic control of plant diversity. *Glob. Ecol. Biogeogr.* **29**, 1634–1650 (2020).

10. C. M. Prager, S. Naeem, N. T. Boelman, J. U. H. Eitel, H. E. Greaves, M. A. Heskel, T. S. Magney, D. N. L. Menge, L. A. Vierling, K. L. Griffin, A gradient of nutrient enrichment reveals nonlinear impacts of fertilization on Arctic plant diversity and ecosystem function. *Ecol. Evol.* **7**, 2449–2460 (2017).

11. B. Holzinger, K. Hülber, M. Camenisch, G. Grabherr, Changes in plant species richness over the last century in the eastern Swiss Alps: elevational gradient, bedrock effects and migration rates. *Plant Ecol.* **195**, 179–196 (2008).

12. G. Arnesen, P. S. A. Beck, T. Engelskjøn, Soil acidity, content of carbonates, and available phosphorus are the soil factors best correlated with alpine vegetation: Evidence from Troms, north Norway. *Arct. Antarct. Alp. Res.* **39**, 189–199 (2007).

13. H. J. B. Birks, V. A. Felde, A. W. R. Seddon, Biodiversity trends within the Holocene. *Holocene*. **26**, 994–1001 (2016).

14. P. Sjögren, C. Damm, Holocene vegetation change in northernmost Fennoscandia and the impact on prehistoric foragers 12 000–2000 cal. a BP – A review. *Boreas*. **48**, 20–35 (2019).

15. J. A. Matthews, A. E. Vater, Pioneer zone geo-ecological change: Observations from a chronosequence on the Storbreen glacier foreland, Jotunheimen, southern Norway. *CATENA*. **135**, 219–230 (2015).

16. L. Stewart, I. G. Alsos, C. Bay, A. L. Breen, C. Brochmann, N. Boulanger-Lapointe, O. Broennimann, H. Bültmann, P. K. Bøcher, C. Damgaard, F. J. A. Daniëls, D. Ehrich, P. B. Eidesen, A. Guisan, I. S. Jónsdóttir, J. Lenoir, P. C. le Roux, E. Lévesque, M. Luoto, J. Nabe-

Nielsen, P. Schönswetter, A. Tribsch, L. U. Tveraabak, R. Virtanen, D. A. Walker, K. B. Westergaard, N. G. Yoccoz, J.-C. Svenning, M. Wisz, N. M. Schmidt, L. Pellissier, The regional species richness and genetic diversity of Arctic vegetation reflect both past glaciations and current climate. *Glob. Ecol. Biogeogr.* **25**, 430–442 (2016).

17. D. A. Fordham, S. T. Jackson, S. C. Brown, B. Huntley, B. W. Brook, D. Dahl-Jensen, M. T. P. Gilbert, B. L. Otto-Bliesner, A. Svensson, S. Theodoridis, J. M. Wilmshurst, J. C. Buettel, E. Canteri, M. McDowell, L. Orlando, J. Pilowsky, C. Rahbek, D. Nogues-Bravo, Using paleo-archives to safeguard biodiversity under climate change. *Science*. **369** (2020), doi:10.1126/science.abc5654.

18. K. J. Willis, K. D. Bennett, S. A. Bhagwat, H. J. B. Birks, 4 °C and beyond: what did this mean for biodiversity in the past? *System. Biodivers.* **8**, 3–9 (2010).

19. T. Giesecke, S. Wolters, J. F. N. van Leeuwen, P. W. O. van der Knaap, M. Leydet, S. Brewer, Postglacial change of the floristic diversity gradient in Europe. *Nat. Commun.* **10**, 5422 (2019).

20. V. A. Felde, J.-A. Grytnes, A. E. Bjune, S. M. Peglar, H. J. B. Birks, Are diversity trends in western Scandinavia influenced by post-glacial dispersal limitation? *J. Veg. Sci*. **29**, 360–370 (2018).

21. H. Seppa, Postglacial trends in palynological richness in the northern Fennoscandian tree-line area and their ecological interpretation. *Holocene*. **8**, 43–53 (1998).

22. T. Giesecke, S. Wolters, S. Jahns, A. Brande, Exploring Holocene changes in palynological richness in northern Europe - did postglacial immigration matter? *PLoS One*. **7**, e51624 (2012).

23. H. J. B. Birks, V. A. Felde, A. E. Bjune, J.-A. Grytnes, H. Seppä, T. Giesecke, Does pollen-assemblage richness reflect floristic richness? A review of recent developments and future

challenges. *Rev. Palaeobot. Palynol.* **228**, 1–25 (2016).

24. L. Parducci, K. D. Bennett, G. F. Ficetola, I. G. Alsos, Y. Suyama, J. R. Wood, M. W. Pedersen, Transley Reviews: Ancient plant DNA from lake sediments. *New Phytol.* **214**, 924–942 (2017).

25. C. L. Clarke, I. G. Alsos, M. E. Edwards, A. Paus, L. Gielly, H. Haflidason, J. Mangerud, P. D. M. Hughes, J. I. Svendsen, A. E. Bjune, A 24,000-year ancient DNA and pollen record from the Polar Urals reveals temporal dynamics of arctic and boreal plant communities. *Quaternary Science Reviews*. **247**, 106564 (2020).

26. P. Sjögren, M. E. Edwards, L. Gielly, C. T. Langdon, I. W. Croudace, M. K. F. Merkel, T. Fonville, I. G. Alsos, Lake sedimentary DNA accurately records 20th Century introductions of exotic conifers in Scotland. *New Phytol.* **213**, 929–941 (2017).

27. S. Liu, K. R. Stoof-Leichsenring, S. Kruse, L. A. Pestryakova, U. Herzschuh, Holocene vegetation and plant diversity changes in the north-eastern Siberian treeline region from pollen and sedimentary ancient DNA. *Frontiers in Ecology and Evolution*. **8**, 304 (2020).

28. I. G. Alsos, Y. Lammers, N. G. Yoccoz, T. Jørgensen, P. Sjögren, L. Gielly, M. E. Edwards, Plant DNA metabarcoding of lake sediments: How does it represent the contemporary vegetation. *PLoS One*. **13**, e0195403 (2018).

29. C. Giguet-Covex, G. F. Ficetola, K. Walsh, J. Poulenard, M. Bajard, L. Fouinat, P. Sabatier, L. Gielly, E. Messager, A. L. Develle, F. David, P. Taberlet, E. Brisset, F. Guiter, R. Sinet, F. Arnaud, New insights on lake sediment DNA from the catchment: importance of taphonomic and analytical issues on the record quality. *Sci. Rep.* **9**, 14676 (2019).

30. E. Willerslev, J. Davison, M. Moora, M. Zobel, E. Coissac, M. E. Edwards, E. D. Lorenzen, M. Vestergård, G. Gussarova, J. Haile, J. Craine, L. Gielly, S. Boessenkool, L. S. Epp, P. B. Pearman,

R. Cheddadi, D. Murray, K. A. Bråthen, N. Yoccoz, H. Binney, C. Cruaud, P. Wincker, T. Goslar, I. G. Alsos, E. Bellemain, A. K. Brysting, R. Elven, J. H. Sønstebø, J. Murton, A. Sher, M. Rasmussen, R. Rønn, T. Mourier, A. Cooper, J. Austin, P. Möller, D. Froese, G. Zazula, F. Pompanon, D. Rioux, V. Niderkorn, A. Tikhonov, G. Savvinov, R. G. Roberts, R. D. E. MacPhee, M. T. P. Gilbert, K. H. Kjær, L. Orlando, C. Brochmann, P. Taberlet, Fifty thousand years of Arctic vegetation and megafaunal diet. *Nature*. **506**, 47–51 (2014).

31. S. M. Otterå, thesis, University of Bergen (2012).

32. S. Shirazi, R. Meyer, B. Shapiro, PCR replication in environmental DNA metabarcoding, , doi:10.22541/au.159309876.62184178.

33. J. Dabney, M. Meyer, S. Pääbo, Ancient DNA damage. *Cold Spring Harb. Perspect. Biol.* **5** (2013), doi:10.1101/cshperspect.a012567.

34. C. L. Clarke, M. E. Edwards, L. Gielly, D. Ehrich, P. D. M. Hughes, L. M. Morozova, H. Haflidason, J. Mangerud, J. I. Svendsen, I. G. Alsos, Persistence of arctic-alpine flora during 24,000 years of environmental change in the Polar Urals. *Sci. Rep.* **9**, 19613 (2019).

35. C. L. Clarke, M. E. Edwards, A. G. Brown, L. Gielly, Y. Lammers, P. D. Heintzman, F. J. Ancin-Murguzur, K.-A. Bråthen, T. Goslar, I. G. Alsos, Holocene floristic diversity and richness in northeast Norway revealed by sedimentary ancient DNA (sedaDNA) and pollen. *Boreas*. **48**, 299–316 (2019).

36. L. H. Voldstad, I. G. Alsos, W. R. Farnsworth, P. D. Heintzman, L. Håkansson, S. E. Kjellman, A. Rouillard, A. Schomacker, P. B. Eidesen, A complete Holocene lake sediment ancient DNA record reveals long-standing high Arctic plant diversity hotspot in northern Svalbard. *Quat. Sci. Rev.* **234**, 106207 (2020).

898 37. C. I. Smith, A. T. Chamberlain, M. S. Riley, A. Cooper, C. B. Stringer, M. J. Collins, Not just old
899 but old and cold? *Nature*. **410**, 771–772 (2001).

900 38. L. Orlando, A. Ginolhac, G. Zhang, D. Froese, A. Albrechtsen, M. Stiller, M. Schubert, E.
901 Cappellini, B. Petersen, I. Moltke, P. L. F. Johnson, M. Fumagalli, J. T. Vilstrup, M. Raghavan, T.
902 Korneliussen, A.-S. Malaspinas, J. Vogt, D. Szklarczyk, C. D. Kelstrup, J. Vinther, A. Dolocan, J.
903 Stenderup, A. M. V. Velazquez, J. Cahill, M. Rasmussen, X. Wang, J. Min, G. D. Zazula, A.
904 Seguin-Orlando, C. Mortensen, K. Magnussen, J. F. Thompson, J. Weinstock, K. Gregersen, K. H.
905 Røed, V. Eisenmann, C. J. Rubin, D. C. Miller, D. F. Antczak, M. F. Bertelsen, S. Brunak, K. A.
906 S. Al-Rasheid, O. Ryder, L. Andersson, J. Mundy, A. Krogh, M. T. P. Gilbert, K. Kjær, T.
907 Sicheritz-Ponten, L. J. Jensen, J. V. Olsen, M. Hofreiter, R. Nielsen, B. Shapiro, J. Wang, E.
908 Willerslev, Recalibrating Equus evolution using the genome sequence of an early Middle
909 Pleistocene horse. *Nature*. **499**, 74–78 (2013).

910 39. K. Hall, C. E. Thorn, N. Matsuoka, A. Prick, Weathering in cold regions: some thoughts and
911 perspectives. *Progress in Physical Geography: Earth and Environment*. **26**, 577–603 (2002).

912 40. K. A. Bråthen, V. T. Ravolainen, Niche construction by growth forms is as strong a predictor of
913 species diversity as environmental gradients. *J. Ecol.* **103**, 701–713 (2015).

914 41. L. Gough, G. R. Shaver, J. Carroll, D. L. Royer, J. A. Laundre, Vascular plant species richness in
915 Alaskan arctic tundra: the importance of soil pH. *J. Ecol.* **88**, 54–66 (2000).

916 42. H. H. Birks, V. J. Jones, S. J. Brooks, H. J. B. Birks, R. J. Telford, S. Juggins, S. M. Peglar, From
917 cold to cool in northernmost Norway: Lateglacial and early Holocene multi-proxy environmental
918 and climate reconstructions from Jansvatnet, Hammerfest. *Quat. Sci. Rev.* **33**, 100–120 (2012).

919 43. B. Huntley, A. J. Long, J. R. M. Allen, Spatio-temporal patterns in Lateglacial and Holocene

vegetation and climate of Finnmark, northernmost Europe. *Quat. Sci. Rev.* **70**, 158–175 (2013).

44. L. Pellissier, K. Anne Bråthen, J. Pottier, C. F. Randin, P. Vittoz, A. Dubuis, N. G. Yoccoz, T. Alm, N. E. Zimmermann, A. Guisan, Species distribution models reveal apparent competitive and facilitative effects of a dominant species on the distribution of tundra plants. *Ecography* . **33**, 1004–1014 (2010).

45. C. K. Ballantyne, A general model of paraglacial landscape response. *Holocene*. **12**, 371–376 (2002).

46. H. H. Birks, South to north: Contrasting late-glacial and early-Holocene climate changes and vegetation responses between south and north Norway. *Holocene*. **25**, 37–52 (2015).

47. C. Jensen, K.-D. Vorren, Holocene vegetation and climate dynamics of the boreal alpine ecotone of northwestern Fennoscandia. *J. Quat. Sci.* **23**, 719–743 (2008).

48. B. Pears, A. G. Brown, P. S. Toms, J. Wood, D. Sanderson, R. Jones, A sub-centennial-scale optically stimulated luminescence chronostratigraphy and late Holocene flood history from a temperate river confluence. *Geology*. **48**, 819–825 (2020).

49. J. H. Sønstebø, L. Gielly, A. K. Brysting, R. Elven, M. Edwards, J. Haile, E. Willerslev, E. Coissac, D. Rioux, J. Sannier, Others, Using next-generation sequencing for molecular reconstruction of past Arctic vegetation and climate. *Mol. Ecol. Resour.* **10**, 1009–1018 (2010).

50. I. Hanssen-Bauer, P. Ø. Nordli, Annual and seasonal temperature variations in Norway 1876-1997. *DNMI report.* **25**, 98 (1998).

51. I. Hanssen-Bauer, E. Førland, Temperature and precipitation variations in Norway 1900--1994 and their links to atmospheric circulation. *International Journal of Climatology: A Journal of the Royal*

Meteorological Society. **20**, 1693–1708 (2000).

52. D. A. Walker, Hierarchical subdivision of Arctic tundra based on vegetation response to climate, parent material and topography. *Glob. Chang. Biol.* **6**, 19–34 (2000).

53. H. Bahlburg, N. Dobrzinski, A review of the Chemical Index of Alteration (CIA) and its application to the study of Neoproterozoic glacial deposits and climate transitions. *Geological Society, London, Memoirs*. **36**, 81–92 (2011).

54. A. Nesje, A piston corer for lacustrine and marine sediments. *Arctic and Alpine Research*. **24**, 257–259 (1992).

55. H. E. Wittmeier, J. Bakke, K. Vasskog, M. Trachsel, Reconstructing Holocene glacier activity at Langfjordjøkelen, Arctic Norway, using multi-proxy fingerprinting of distal glacier-fed lake sediments. *Quaternary Science Reviews*. **114**, 78–99 (2015).

56. F. Bogren, thesis, Stockholm University (2019).

57. O. Heiri, A. F. Lotter, G. Lemcke, Loss on ignition as a method for estimating organic and carbonate content in sediments: reproducibility and comparability of results. *J. Paleolimnol.* **25**, 101–110 (2001).

58. T. Goslar, J. Czernik, E. Goslar, Low-energy 14C AMS in Poznań Radiocarbon Laboratory, Poland. *Nuclear Instruments and Methods in Physics Research Section B: Beam Interactions with Materials and Atoms*. **223-224**, 5–11 (2004).

59. M. Blaauw, J. Andrés Christen, Flexible paleoclimate age-depth models using an autoregressive gamma process. *Bayesian Analysis*. **6**, 457–474 (2011).

60. R Core Team, *R: A language and environment for statistical computing* (2019).

962 61. P. J. Reimer, E. Bard, A. Bayliss, J. Warren Beck, P. G. Blackwell, C. B. Ramsey, C. E. Buck, H.
963 Cheng, R. Lawrence Edwards, M. Friedrich, P. M. Grootes, T. P. Guilderson, H. Haflidason, I.
964 Hajdas, C. Hatté, T. J. Heaton, D. L. Hoffmann, A. G. Hogg, K. A. Hughen, K. Felix Kaiser, B.
965 Kromer, S. W. Manning, M. Niu, R. W. Reimer, D. A. Richards, E. Marian Scott, J. R. Southon,
966 Richard A Staff, C. S. M. Turney, J. van der Plicht, IntCal13 and Marine13 radiocarbon age
967 calibration curves 0–50,000 years cal BP. *Radiocarbon*. **55**, 1869–1887 (2013).

968 62. H. H. Zimmermann, E. Raschke, L. S. Epp, K. R. Stoof-Leichsenring, G. Schwamborn, L.
969 Schirrmeister, P. P. Overduin, U. Herzschuh, Sedimentary ancient DNA and pollen reveal the
970 composition of plant organic matter in Late Quaternary permafrost sediments of the Buor Khaya
971 Peninsula (north-eastern Siberia). *Biogeosciences*. **14**, 575–596 (2017).

972 63. I. G. Alsos, P. Sjögren, A. G. Brown, L. Gielly, M. K. F. Merkel, A. Paus, Y. Lammers, M. E.
973 Edwards, T. Alm, M. Leng, T. Goslar, C. T. Langdon, J. Bakke, W. G. M. van der Bilt, Last
974 Glacial Maximum environmental conditions at Andøya, northern Norway; evidence for a northern
975 ice-edge ecological "hotspot." *Quaternary Science Reviews*. **239**, 106364 (2020).

976 64. P. Taberlet, E. Coissac, F. Pompanon, L. Gielly, C. Miquel, A. Valentini, T. Vermat, G. Corthier,
977 C. Brochmann, E. Willerslev, Power and limitations of the chloroplast trnL (UAA) intron for plant
978 DNA barcoding. *Nucleic Acids Res.* **35**, e14 (2007).

979 65. P. Taberlet, A. Bonin, L. Zinger, E. Coissac, Environmental DNA. *Oxford Scholarship Online*
980 (2018), , doi:10.1093/oso/9780198767220.001.0001.

981 66. F. Boyer, C. Mercier, A. Bonin, Y. Le Bras, P. Taberlet, E. Coissac, OBITOOLS: a unix-inspired
982 software package for DNA metabarcoding. *Mol. Ecol. Resour.* **16**, 176–182 (2016).

983 67. E. M. Soininen, G. Gauthier, F. Bilodeau, D. Berteaux, L. Gielly, P. Taberlet, G. Gussarova, E.

Bellemain, K. Hassel, H. K. Stenøien, L. Epp, A. Schrøder-Nielsen, C. Brochmann, N. G. Yoccoz, Highly overlapping winter diet in two sympatric lemming species revealed by DNA metabarcoding. *PLoS One*. **10**, e0115335 (2015).

68. R. Elven, D. F. Murray, V. Y. Razzhivin, B. A. Yurtsev, *Annotated checklist of the panarctic flora (PAF) vascular plants* (Natural History Museum, University of Oslo, 2011).

69. R. Elven, T. Alm, T. Berg, J. I. I. Båtvik, E. Fremstad, O. Pedersen, *Johannes Lid & Dagny Tande Lid: Norsk flora* (Det Norske Samlaget, 2005).

70. M. O. Hill, Diversity and evenness: a unifying notation and its consequences. *Ecology*. **54**, 427–432 (1973).

71. A. Chao, N. J. Gotelli, T. C. Hsieh, E. L. Sander, K. H. Ma, R. K. Colwell, A. M. Ellison, Rarefaction and extrapolation with Hill numbers: a framework for sampling and estimation in species diversity studies. *Ecol. Monogr.* **84**, 45–67 (2014).

72. W. Chen, G. F. Ficetola, Numerical methods for sedimentary-ancient-DNA-based study on past biodiversity and ecosystem functioning. *Environmental DNA.* **2**, 115–129 (2020).

73. S. N. Wood, *Generalized Additive Models: An Introduction with R* (CRC Press, ed. 2, 2017).

74. T. Hastie, R. Tibshirani, Generalized additive models. *Stat. Sci.* **1**, 297–318 (1986).

75. G. L. Simpson, Modelling palaeoecological time series using generalised additive models. *Frontiers in Ecology and Evolution*. **6**, 149 (2018).

76. M. Walker, P. Gibbard, M. J. Head, M. Berkelhammer, S. Björck, H. Cheng, L. C. Cwynar, D. Fisher, V. Gkinis, A. Long, J. Lowe, R. Newnham, S. O. Rasmussen, H. Weiss, Formal Subdivision of the Holocene Series/Epoch: A Summary. *Journal of the Geological Society of*

India. **93**, 135–141 (2019).

77. J. Oksanen, F. G. Blanchet, M. Friendly, R. Kindt, P. Legendre, D. McGlinn, P. R. Minchin, R. B. O'Hara, G. L. Simpson, P. Solymos, M. H. H. Stevens, E. Szoecs, H. Wagner, *vegan: Community Ecology Package* (2019).

78. H. Wickham, *ggplot2: Elegant Graphics for Data Analysis* (Springer, 2016).

79. A. L. C. Hughes, R. Gyllencreutz, Ø. S. Lohne, J. Mangerud, J. I. Svendsen, The last Eurasian ice sheets – a chronological database and time-slice reconstruction, DATED-1. *Boreas*. **45**, 1–45 (2016).

80. K. K. Andersen, N. Azuma, J.-M. Barnola, M. Bigler, P. Biscaye, N. Caillon, J. Chappellaz, H. B. Clausen, D. Dahl-Jensen, H. Fischer, J. Flückiger, D. Fritzsche, Y. Fujii, K. Goto-Azuma, K. Grønvold, N. S. Gundestrup, M. Hansson, C. Huber, C. S. Hvidberg, S. J. Johnsen, U. Jonsell, J. Jouzel, S. Kipfstuhl, A. Landais, M. Leuenberger, R. Lorrain, V. Masson-Delmotte, H. Miller, H. Motoyama, H. Narita, T. Popp, S. O. Rasmussen, D. Raynaud, R. Rothlisberger, U. Ruth, D. Samyn, J. Schwander, H. Shoji, M.-L. Siggard-Andersen, J. P. Steffensen, T. Stocker, A. E. Sveinbjörnsdóttir, A. Svensson, M. Takata, J.-L. Tison, T. Thorsteinsson, O. Watanabe, F. Wilhelms, J. W. C. White, North Greenland Ice Core Project members, High-resolution record of Northern Hemisphere climate extending into the last interglacial period. *Nature*. **431**, 147–151 (2004).

Acknowledgements

General: We thank Roseanna Mayfield and Kristian Sirkka for assistance with fieldwork; Marie Føreid Merkel, Sandra Garces Pastor, and Yann Belov for technical assistance in the lab; Karina Monsen for assistance with high-resolution photography; Eivind Støren, Department of Earth Science, University of Bergen for providing access to cold rooms and helping to locate and transport cores; Ruth Paulssen and the Genomics Support Centre Tromsø (GSCT) at UiT-The Arctic University of Norway for amplicon sequencing; Dorothee Ehrich for fruitful discussions and coring at Sandfjorddalen; Matthias Forwick for help organizing scanning of cores; and Lasse Topstad and Leif Einar Støvern for providing photographs. DPR is thankful to Keshav Prasad Paudel for his help in map creation. Bioinformatic analyses were performed on resources provided by UNINETT Sigma2 - the National Infrastructure for High Performance Computing and Data Storage in Norway.

Funding: The study is part of the project "ECOGEN - Ecosystem change and species persistence over time: a genome-based approach", which is financed by Research Council of Norway grant number 250963/F20.

Author contributions: IGA, KAB, NGY, TA, and MEE designed the research and raised the funding; IGA, AGB, DPR, PDH, FJAM, YL, KAB and KEL did the fieldwork; JB, KFH, and JSS provided resources; DPR, PDH, KEL and IP did the laboratory work with input from IGA and AGB; TG performed radiocarbon dating; PDH built composite cores and performed age-depth modelling with input from AGB, TG and KFH; YL and PDH designed the bioinformatic pipeline with input from DPR and IGA; IGA and DPR verified and curated barcode taxonomic assignments; PDH and YL designed and performed the quality control checks with input from DPR and IGA; DPR did the statistical analyses with input from NGY and KAB; YL, DPR and PDH curated the data; DPR, PDH, AGB and IGA drafted the manuscript; and all authors have reviewed and approved the final manuscript.

Competing interests: The authors declare no competing interests.

Data and materials availability: Raw sequence data have been deposited in the European Nucleotide Archive (ENA) at project accession PRJEB39329, with sample accessions ERS4812035-ERS4812048. All radiocarbon, loss-on-ignition, and processed sedaDNA data are available in the Supplementary Materials. Pre-filtered ObiTools tsv output files have been uploaded to figshare (DOI: [available upon acceptance]). Scripts are on Github with URLs cited in the Materials and Methods section.

1052 **Figures**

1053

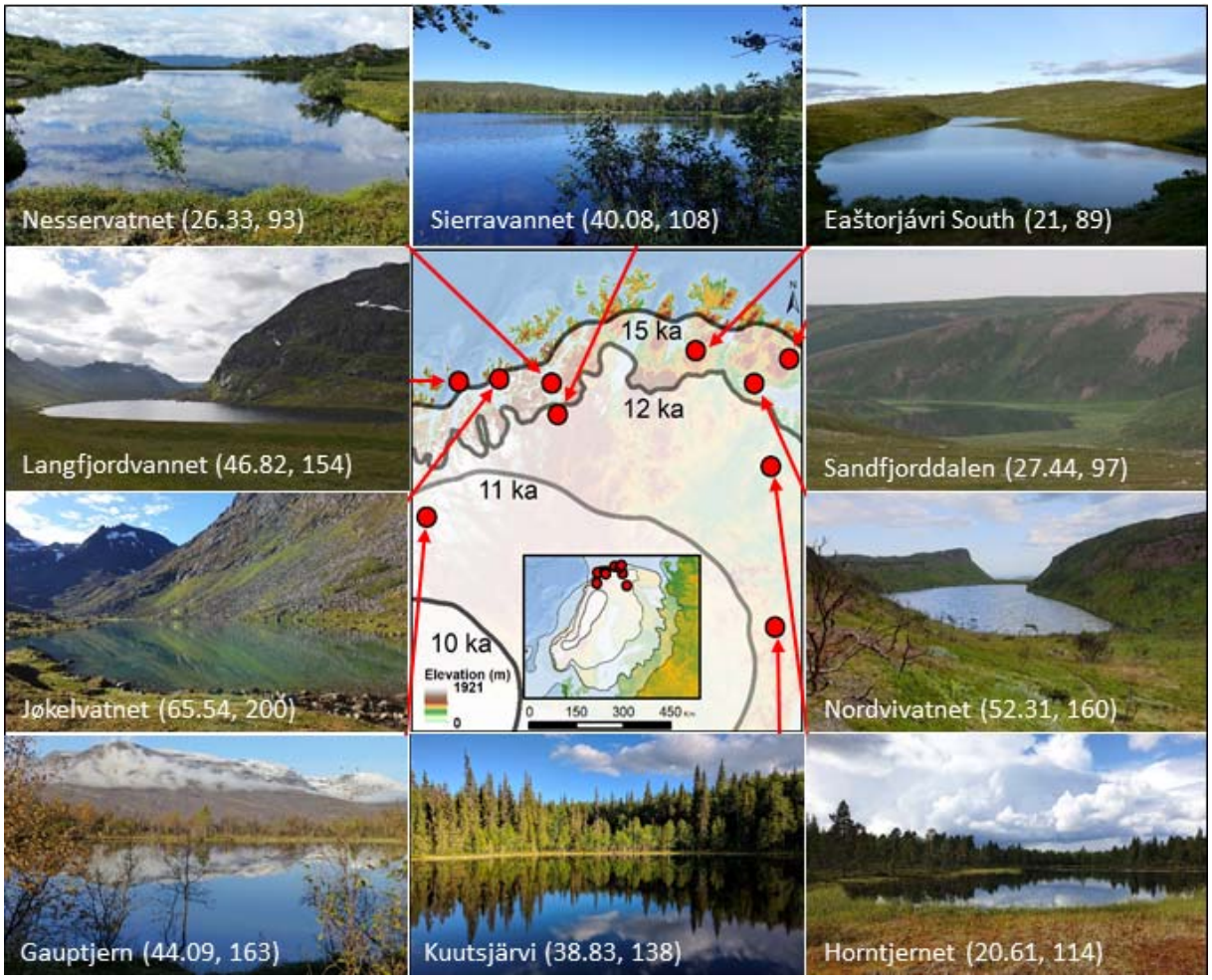

1054

1055 **Fig. 1. Geographical setting of the study area and images of the ten lakes**. The extent of the
1056 Scandinavian ice sheet (the most credible extent of *79*) at 21.0 (inset only), 15.0, 12.0, 11.0, and 10.0
1057 ka are indicated by semi-transparent layers. Lake names are followed by mean taxonomic richness and
1058 total taxa recorded in each lake (local species pool). See Data set S1 for further site information. Map
1059 data source: European Environment Agency; photo credits: Jøkelvatnet, Lasse Topstad;
1060 Sandfjorddalen, Leif Einar Støvern; Langfjordvannet & Eaštorjávri South, Dilli P. Rijal; Kuutsjärvi,
1061 Karin Helmens; all others, Inger G. Alsos.

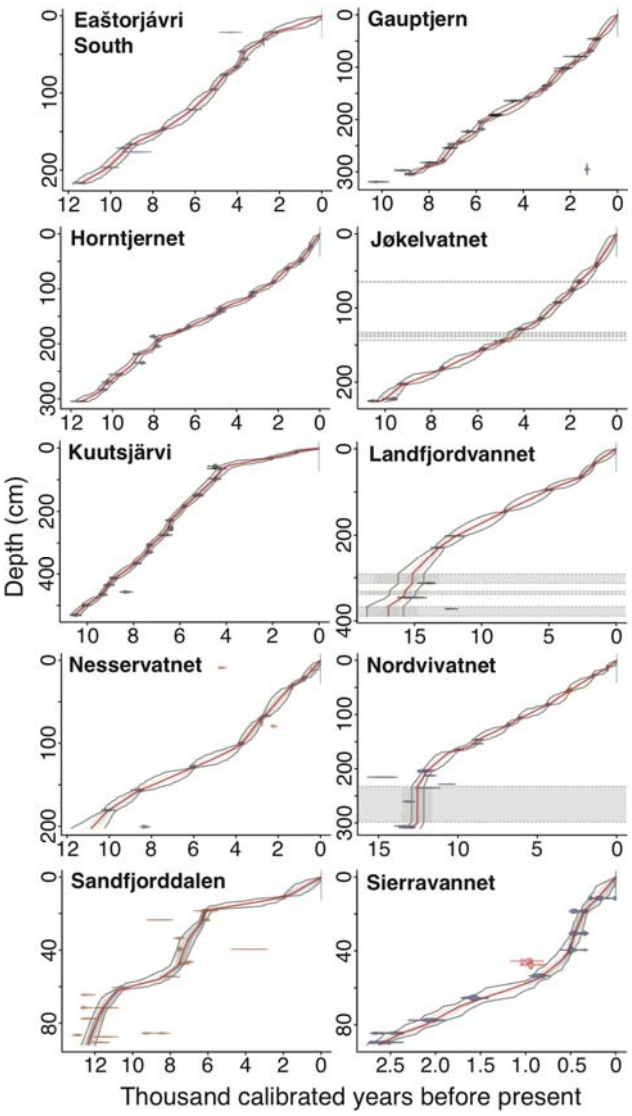

1062

1063 **Fig. 2. Bayesian age-depth models for ten lakes from northern Fennoscandia**. Colors for calibrated
1064 radiocarbon dates follow Fig. S1. Excluded dates are in red, and inferred slumps are shown with grey
1065 shading. Median modelled ages are indicated by the redlines, with the bubbles representing 95%
1066 credibility intervals.

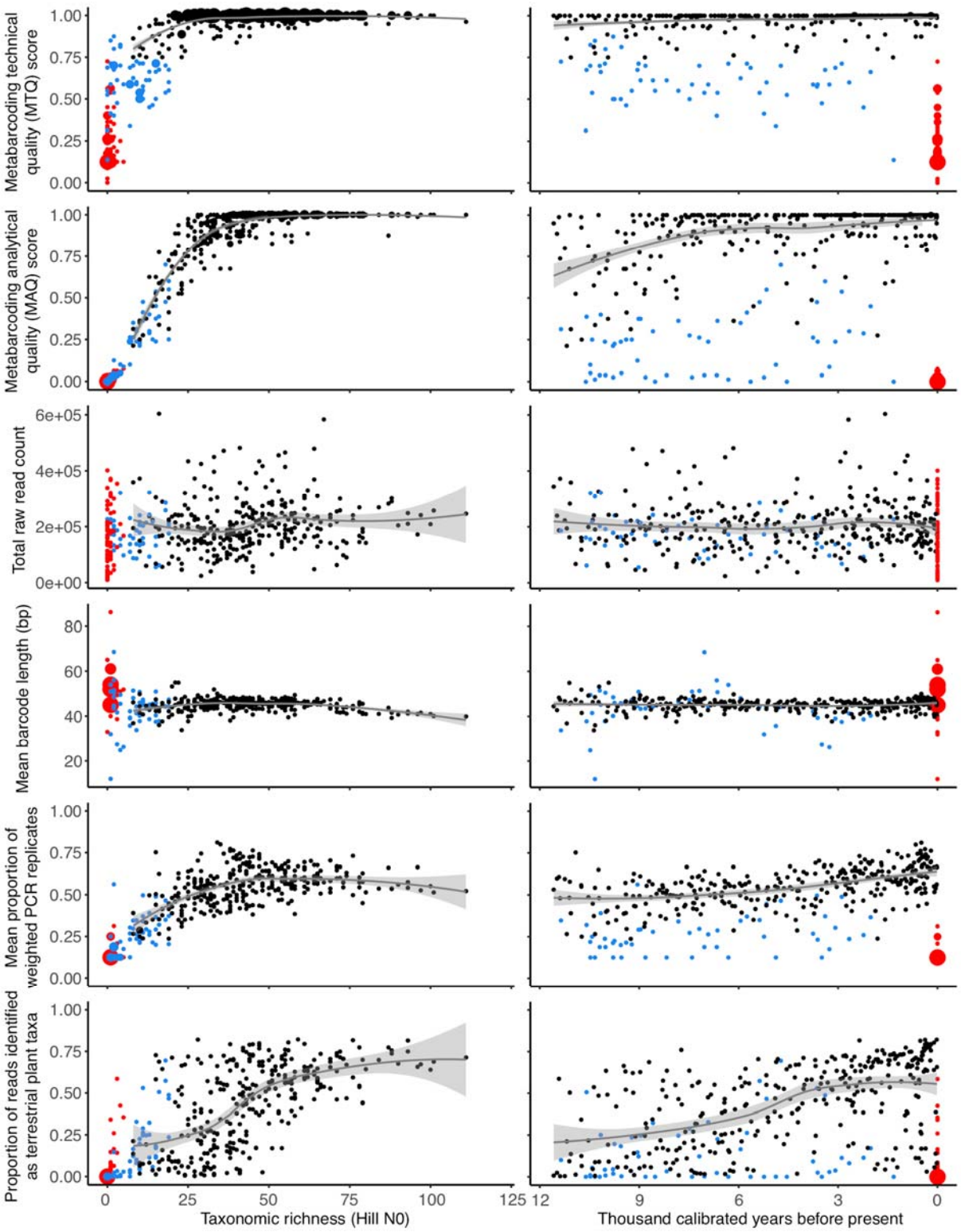

Fig. 3. Correlations between observed taxonomic richness (left panels) and time (right panels) against six measures of *sed*aDNA data quality. Sample age minimally impacts *metabarcoding*

1070 *technical quality (MTQ)* and *metabarcoding analytical quality (MAQ)* scores, total raw read count,
1071 mean barcode length, and the mean proportion of weighted PCR replicates (*wtRep*) across the entire
1072 data set, although the proportion of reads identified as terrestrial plant increases through time. Data in
1073 black, samples that passed quality control (QC); blue, samples that failed QC; red, negative controls.
1074 Fitted loess-smoothed lines along with one standard error envelope are for samples that passed QC.
1075 Data for individual lakes are presented in Fig. S4.

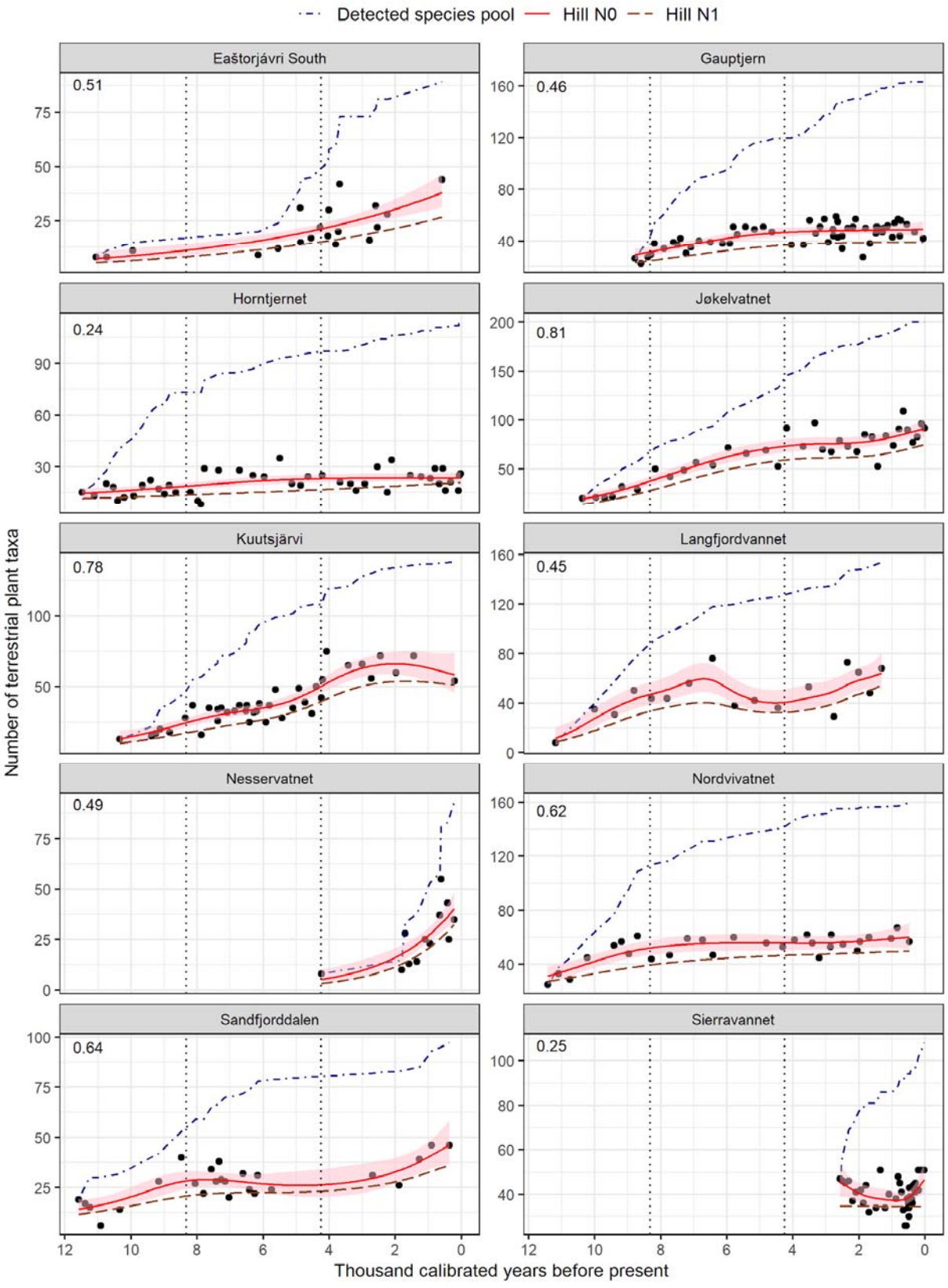

1076

Fig. 4. Holocene patterns of local terrestrial plant richness in 10 lake catchments from northern Fennoscandia. The predicted values for observed taxonomic richness (Hill N0) are based on the generalized additive mixed models (GAMM; solid red line) along with 95% confidence intervals in pink shading. Numbers in the top-left corner of each plot represent adjusted R-square values for the GAMMs. The fitted lines for Hill N1 are indicated by a dashed brown line. The development of local species pools are expressed in terms of detected cumulative count of taxa (blue dot-dashed line) through time. The Early (11.7-8.3 ka), Middle (8.3-4.25 ka), and Late Holocene (4.25-0.0 ka) periods are indicated by vertical dotted lines. Note difference in scale on the y-axes.

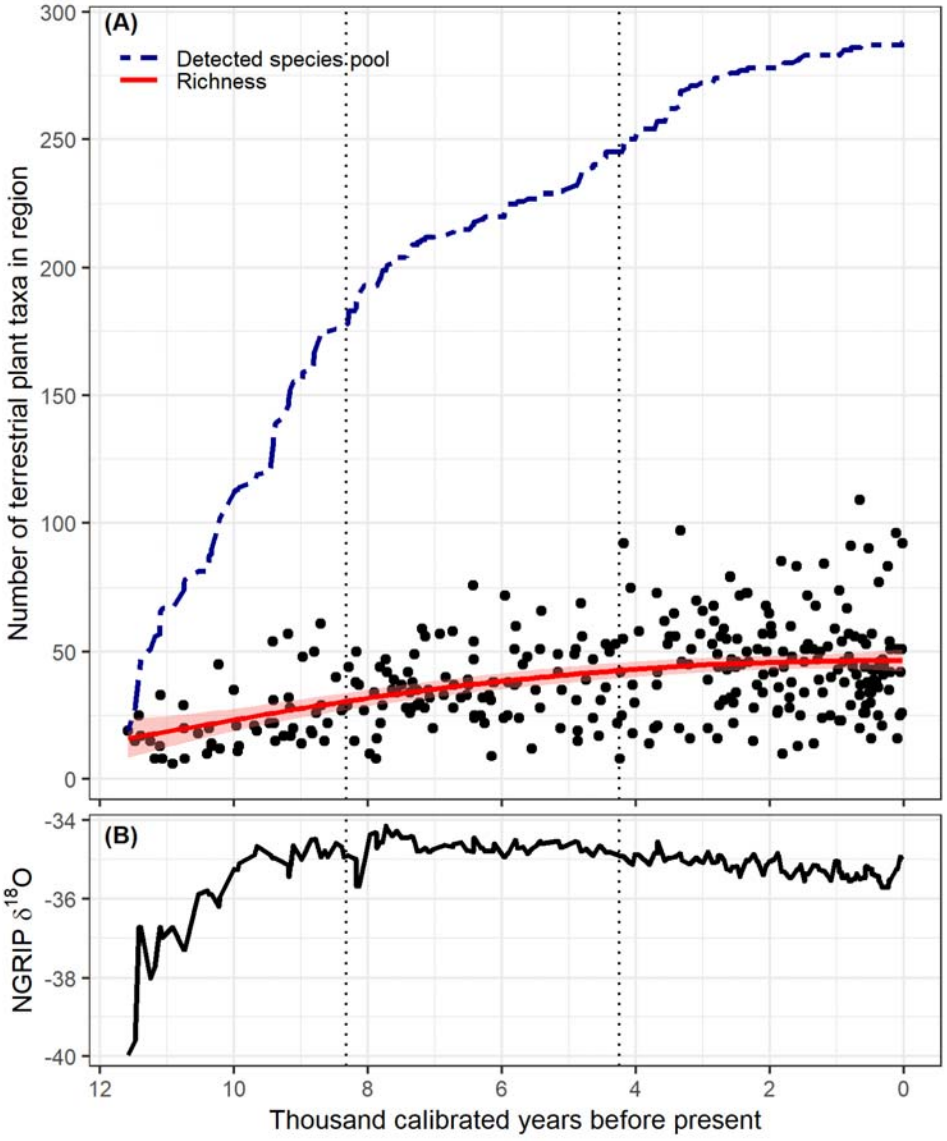

Fig. 5. The accumulated regional species pool, taxonomic richness of each sample, and NGRIP temperature proxy across the Holocene of northern Fennoscandia. (**A**) accumulation of the detected regional species pool (defined as cumulative number of taxa; double-dashed line) as well as number of taxa detected per sample (n=316) along with the 95% confidence interval (pink shading) of the fitted line (solid red line) based on a generalized additive model, and (**B**) variation in temperature reflected by North Greenland Ice Core Project (NGRIP) $\delta^{18}O$ values (*80*), with temperature being positively correlated with $\delta^{18}O$ values. The overall patterns remain the same if two shorter cores

1093 spanning only the Late Holocene are excluded (Fig. S6). The Early (12.0-8.3 ka), Middle (8.3-4.25 ka),

1094 and Late Holocene (4.25-0.0 ka) periods are indicated by dotted vertical lines.

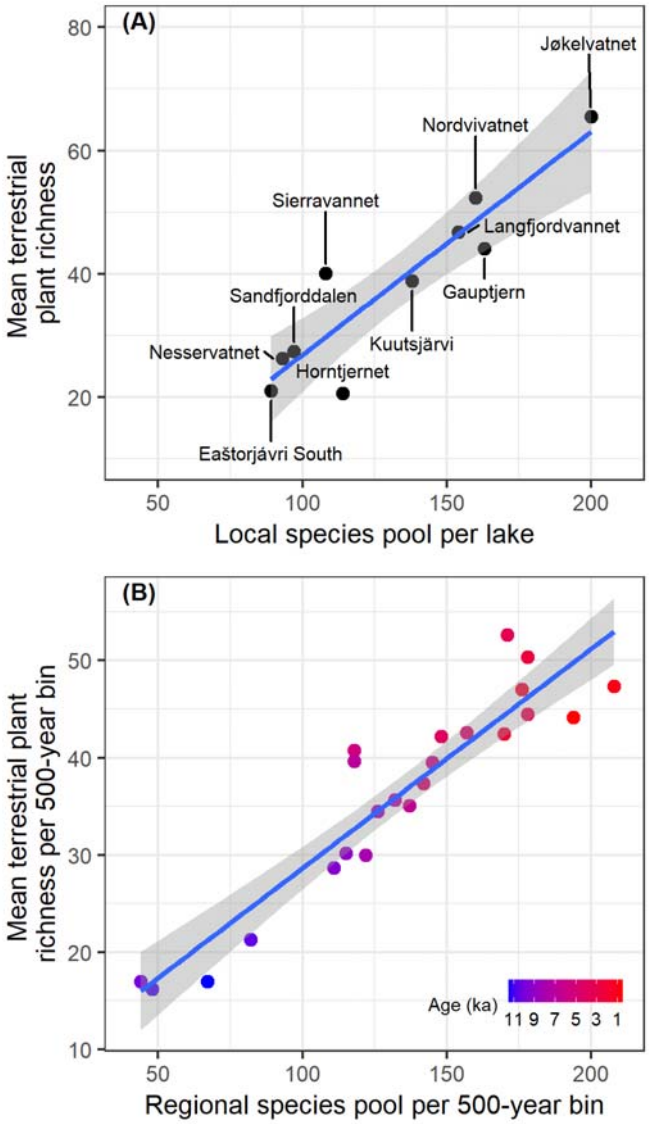

Fig. 6. Relationship between species pool and taxonomic richness. Correlation between (**A**) local species pool (total number of taxa observed over the Holocene for individual lakes) or (**B**) regional species pool (total number of taxa observed per 500-year time bin) and the respective mean taxonomic richness of terrestrial plants in northern Fennoscandia.

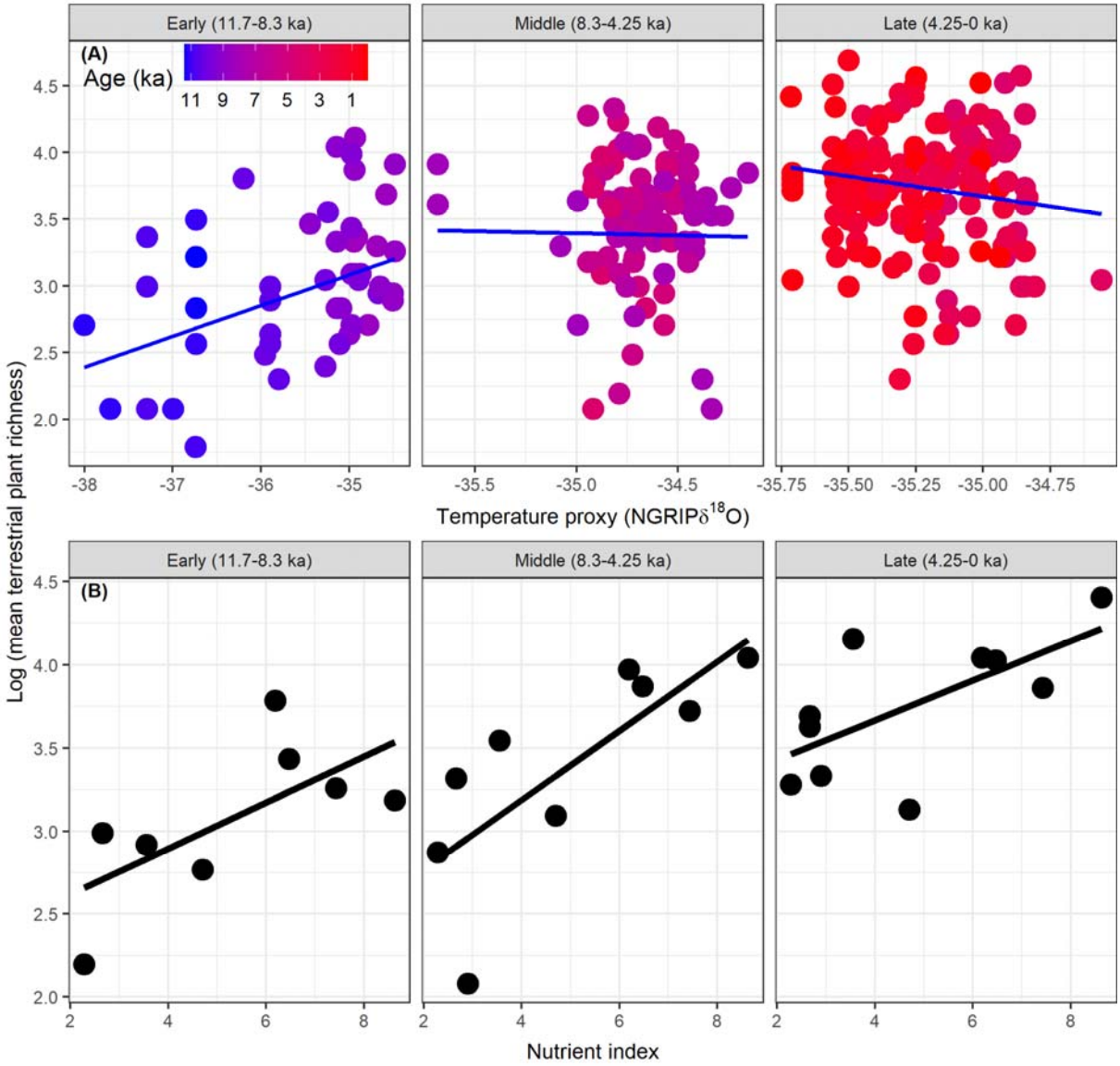

Fig. 7. Impact of climate and nutrient index on observed terrestrial plant taxonomic richness. (**A**) Linear mixed effect model showing the impact of regional climate on taxonomic richness of terrestrial plants for three periods of the Holocene. Temperature is positively correlated with $\delta^{18}O$ values. Two samples with NGRIP $\delta^{18}O$ lower than -39 were not included in the analysis. Note difference in scale on x-axes. (**B**) Linear models showing spatial patterns of mean taxonomic richness of terrestrial plants with the nutrient index for three periods of the Holocene.